

**RipAY, a plant pathogen effector protein exhibits robust  $\gamma$ -glutamyl cyclotransferase activity when stimulated by eukaryotic thioredoxins**

Shoko Fujiwara<sup>1</sup>, Tomoki Kawazoe<sup>1</sup>, Kouhei Ohnishi<sup>2</sup>, Takao Kitagawa<sup>3</sup>, Crina Popa<sup>4</sup>, Marc Valls<sup>4</sup>, Stéphane Genin<sup>5</sup>, Kazuyuki Nakamura<sup>6</sup>, Yasuhiro Kuramitsu<sup>3</sup>, Naotaka Tanaka<sup>1</sup> & Mitsuaki Tabuchi<sup>1,7</sup>

<sup>1</sup> Department of Applied Biological Science, Faculty of Agriculture, Kagawa University, Miki-cho, Kagawa, 761-0795, Japan.

<sup>2</sup> Research Institute of Molecular Genetics, Kochi University, Nankoku, 783-0093, Japan.

<sup>3</sup> Department of Biochemistry and Functional Proteomics, Yamaguchi University Graduate School of Medicine, Ube, Yamaguchi, 755-8505, Japan.

<sup>4</sup> Departament de Genètica, Universitat de Barcelona and Centre for Research in Agricultural Genomics (CSIC-IRTA-UB-UAB), Bellaterra, Catalonia, Spain.

<sup>5</sup> INRA-CNRS, Laboratoire des Interactions Plantes-Microorganismes (LIPM), UMR441-2594, Castanet-Tolosan, France.

<sup>6</sup> Center of Clinical Laboratories in Tokuyama Medical Association Hospital, Shunan, 745-0846, Japan.

\*Running title: *γ-Glutamyl cyclotransferase activated by eukaryotic thioredoxins*

<sup>7</sup>To whom correspondence should be addressed: Mitsuaki Tabuchi, Dept. of Applied Biological Science, Faculty of Agriculture, Kagawa University, 2393 Ikenobe Miki-cho, Kagawa 761-0795, Japan, Tel: +81-87-891-3110; Fax: +81-87-891-3021; E-mail: [mtabuchi@ag.kagawa-u.ac.jp](mailto:mtabuchi@ag.kagawa-u.ac.jp)

**Keywords:** pathogen effector; type III secretion system (T3SS); plant pathogenic bacterium; *Ralstonia solanacearum*; *Saccharomyces cerevisiae*; glutathione; gamma-glutamyl cyclotransferase; ChaC ; thioredoxin

**ABSTRACT**

The plant pathogenic bacterium *Ralstonia solanacearum* injects more than 70 effector proteins (virulence factors) into the host plant cells via the needle-like structure of a type III secretion system (T3SS). The T3SS effector proteins manipulate host regulatory networks to suppress defense responses with diverse molecular activities. Uncovering the molecular function of these effectors is essential for a mechanistic understanding of *R. solanacearum* pathogenicity. However, few of the effectors from *R. solanacearum* have been functionally characterized and their plant targets remain largely unknown. Here, we show that the ChaC-domain containing effector RipAY/RSp1022 from *R. solanacearum* exhibits  $\gamma$ -glutamyl cyclotransferase (GGCT) activity to degrade the major intracellular redox buffer, glutathione. Heterologous expression of RipAY, but not other ChaC family proteins conserved in various organisms caused growth inhibition to yeast *Saccharomyces cerevisiae*, and the intracellular

glutathione level was decreased to approximately 30% of the normal level following expression of RipAY in yeast. Although active site mutants of GGCT activity were non-toxic, addition of glutathione did not reverse the toxicity suggesting that the toxicity might be a consequence of activity against other  $\gamma$ -glutamyl-compounds. Intriguingly, RipAY protein purified from a bacterial expression system did not exhibit any GGCT activity, whereas it exhibited robust GGCT activity upon its interaction with eukaryotic thioredoxins, which are important for intracellular redox homeostasis during bacterial infection in plants. Our results suggest that RipAY has evolved to sense the host intracellular redox environment, which triggers its enzymatic activity to create a favorable environment for *R. solanacearum*-infection.

Numerous bacterial pathogens of plants and animals inject virulence proteins, so-called effectors, directly into the host cell cytoplasm through specialized secretion apparatuses, such as the type III secretion system (T3SS). The

translocated T3SS effector proteins manipulate diverse host cellular processes including cytoskeletal reorganization, signal transduction, gene expression, vesicular trafficking, autophagy and DNA replication to promote infection and ultimately cause disease (1,2). Although the identification of the biochemical activities of these effector proteins is essential to understand the molecular mechanism of pathogenesis, it has been of great difficulty to predict the molecular functions based on their primary sequences because many effector proteins have limited similarity to known proteins and some effectors can be considered “convergently evolved” mimics of their eukaryotic cell counterparts (3). Furthermore, thanks to extensive genome sequencing programs, coupled with robust computational predictions of sequence motifs characteristic of effector proteins, the number of putative effectors identified in the genomes from many bacterial pathogens is continuously accumulating in the database (4). For the above reasons, a function-based method to efficiently analyze effector proteins is desired. Interestingly, effector proteins have been observed to confer a growth inhibition phenotype when heterologously-expressed in the yeast *Saccharomyces cerevisiae* (5,6). This growth inhibition is thought to be the consequence of the effector-induced compromise of cellular processes conserved between yeast and higher eukaryotes. For example, Lesser and Miller (7) showed that the *Yersinia* effector YopE, which functions as Rho GTPase activating protein (RhoGAP), blocks actin polarization and cell cycle progression through its RhoGAP activity. Importantly, growth inhibition is a genetically tractable phenotype, and it provides a variety of means to investigate modes of action of these effectors toward host cell targets.

*Ralstonia solanacearum*, which is a widely distributed soil-borne phytopathogen, causes lethal bacterial wilt of more than 200 plant species, including economically important crops, such as tomato, potato, and tobacco (8). Among the pathogenicity determinants of this bacterium, T3SS was shown to play an essential role in pathogenicity as the corresponding mutants were avirulent on host plants (9). In general, compared to animal pathogens, bacterial plant pathogens such as *Xanthomonas* spp. or *Pseudomonas*

*syringae* contain larger numbers (~30–40) of effectors, but the *R. solanacearum* effector repertoire is exceptionally large, probably due to its wide host range (10). Post-genomic functional analyses using regulatory-based approaches and/or T3SS-translocon assays have identified the nearly complete repertoire of 70–75 effectors in the reference strain GMI1000 and the phylogenetically close strain RS1000 (11). The investigation of the *R. solanacearum* strain complex (RSSC) pangenome also identified additional families of likely effector proteins with no homology to other previously identified effectors, and thus the current estimated number of effector families is approximately 110 among 11 strains representative of the biodiversity of the RSSC (12). Individual *R. solanacearum* strains typically possess around 60–75 effectors. Effector repertoire comparison revealed a group of 32 core effectors present in 10 of 11 strains (13). To date, only a few of *R. solanacearum* effectors have been assigned molecular functions and targets (14–16), but most of these effectors remain functionally uncharacterized.

In this study, we screened *R. solanacearum* effectors using a yeast expression system and identified RipAY as an effector whose expression causes growth inhibition in yeast. RipAY, which is one of the *R. solanacearum* core effectors, has previously been shown experimentally to be an effector injected into host plant cells via T3SS (17), but the molecular function of this effector has yet to be characterized. Bioinformatics analysis revealed that RipAY contains a ChaC domain, which is a conserved domain found in all phyla examined, but whose molecular function was totally unknown when we started our study. Recently, it has been reported that yeast and mammalian ChaC-domain containing proteins exhibit  $\gamma$ -glutamyl cyclotransferase (GGCT) activity specifically to degrade glutathione (18). We demonstrated that RipAY exhibits robust GGCT activity and significantly decreases intracellular glutathione in yeast. Surprisingly, we failed to detect GGCT activity of recombinant RipAY expressed in *Escherichia coli*. However, we could detect robust GGCT activity when RipAY was activated by yeast or plant thioredoxins. Both glutathione and thioredoxins are important for maintaining cellular redox homeostasis and also indispensable for proper

activation of plant innate immunity during pathogen infection (19,20). Together, our data provide new insights that *R. solanacearum* perturbs the host redox environment to allow bacterial infection.

## EXPERIMENTAL PROCEDURES

**Strains, Plasmids and Media**—Descriptions of the strains and plasmids used in this study are presented in Tables 1, 2, and 3. *Escherichia coli* DB3.1 (Life Technologies) was used for the construction and amplification of the Gateway™ vectors, and *E. coli* DH5α or JM109 was the bacterial host for all the other plasmids constructed. Coding sequences were amplified by PCR using KOD plus neo polymerase (Toyobo) or PrimeSTAR GXL polymerase (Takara Bio). Plasmids were sequenced to ensure that no mutations were introduced due to manipulations. Yeast transformation was performed using the lithium-acetate method (21). Mutant constructs were generated by site-directed mutagenesis (22) and confirmed by sequencing. The media used for yeast culture were synthetic dextrose (SD) medium (2% glucose, 0.67% yeast nitrogen base without amino acids) and synthetic galactose (SGal) medium (2% galactose, 0.67% yeast nitrogen base without amino acids). Appropriate amino acids and bases were added to SD or SGal medium as necessary. Yeast cells were cultured at 26°C unless otherwise stated.

**Phylogenetic Analysis**—Phylogenetic trees of ChaC domain containing proteins including RipAY or thioredoxins from various organisms were created with MEGA6 (23). The amino acid sequences of ChaC proteins or thioredoxins from NCBI database were aligned with CLUSTAL-W, from which a maximum-likelihood phylogenetic tree was created.

**Homology Modeling and Structure Analysis**—The RipAY protein sequence was used for fold recognition using Phyre2 server (<http://www.sbg.bio.ic.ac.uk/phyre2/html/page.cgi?id=index>). This search identified human GGCT (C7 orf24, PDB ID: 2PN7 and 2RBH) as best template. We used the alignment provided by Phyre2 server to construct models for RipAY using CueMol molecular graphics software (<http://www.cuemol.org/ja/>).

**Production and Purification of Recombinant Proteins in *E. coli***—For the purification of the His<sub>6</sub>-tagged recombinant proteins, Rosetta-gami B (DE3) cells (EMD) carrying pET23d-*GCG1*, *DUG1*, RipAY, or *TRX1* plasmid or pDEST17-*TRXA* or -*TRX-h2*, -*h3*, -*h5* or *TRX-h5*<sup>C39, 42S</sup> plasmid were grown in 600 mL of Luria-Bertani (LB) medium with 34 μg/mL chloramphenicol, and 100 μg/mL ampicillin at 37°C to an OD<sub>600</sub> of 0.8. The bacteria were then moved to 18°C for 30 min and the protein expression was induced by the addition of IPTG to 0.3 mM for 6 h. The cells were collected by centrifugation at 10,000 × *g* for 5 min. The cell pellet was resuspended in 30 mL of binding buffer (50 mM NaH<sub>2</sub>PO<sub>4</sub>, 500 mM NaCl, 5 mM imidazole, pH 8.0) containing 1 mM PMSF and disrupted by sonication. The lysate was cleared by centrifugation at 10,000 × *g* for 30 min at 4°C and the cleared lysate was applied to the HisTrap FF 1-mL column (GE healthcare) equilibrated with binding buffer. The column was then washed with 20-column volume of binding buffer and eluted with elution buffer (50 mM NaH<sub>2</sub>PO<sub>4</sub>, 500 mM NaCl, 300 mM imidazole, pH 8.0). Fractions containing the recombinant His<sub>6</sub>-tagged fusion proteins were collected. Purified His<sub>6</sub>-tagged thioredoxins were treated with 20 mM dithiothreitol (DTT) at RT for 15 min to reduce thioredoxins. Purified proteins were subsequently dialyzed into PBS, and protein concentrations were determined using a micro BCA protein assay kit (Thermo Scientific).

**Measurement of Cys-Gly Peptidase (*Dug1*)-coupled GGCT Activity of His<sub>6</sub>-tagged RipAY and Gcg1 Purified from *E. coli***—GGCT activity toward glutathione as substrate was carried out using *Dug1*-coupled assay as previously described (18), with some modifications. In brief, 0.4 μM Gcg1 or 0.04 μM RipAY with appropriate concentrations of the cell lysates from various organisms or thioredoxins purified from *E. coli* was incubated with glutathione for 20 min at 37°C in 50 μL of reaction mixture containing 50 mM Tris-HCl (pH 8.0). The reaction was terminated by addition of 20 μL of 0.25 N HCl and then neutralized with addition of 8.4 μL of 1 M Tris and made up to 100 μL with 50 mM Tris-HCl (pH 8.0). Ten microliters of the reaction mixture was then

transferred to a new tube to which was added 2  $\mu$ L of Dug1 reaction mixture; this converts the Cys-Gly dipeptide into free cysteine and glycine. The Dug1 reaction mixture consisted of 20  $\mu$ M MnCl<sub>2</sub> and 1  $\mu$ g recombinant *S. cerevisiae* Dug1p, a Cys-Gly peptidase purified from *E. coli*. This reaction mixture was further incubated for 1 h at 37°C. The free cysteine generated was measured by acidic ninhydrin solution (20 g ninhydrin dissolved in acetic acid and HCl that are mixed in a 3:2 ratio) were added to the reaction mixture and the reaction mixture incubated at 100°C for 10 min to develop the pink color. Two-hundred microliters of colored solutions was transferred to a 96-well plate and the OD was measured at 570 nm using microplate reader (Bio-Rad). The assay was performed in triplicates and data are mean  $\pm$  SEM.

*Measurement of GGCT Activity of Protein A-tagged RipAY and Gcg1—GCG1, ripAY<sup>WT</sup> or ripAY<sup>E216Q</sup> genes on pDONR221 donor vector were cloned into the protein A-tagging gateway destination vectors, pMT1371 for E. coli or pMT1373 for S. cerevisiae by LR reaction. E. coli Rosetta gami B (DE3) cells carrying pMT1371-GCG1, ripAY<sup>WT</sup>, ripAY<sup>E216Q</sup> or ripAY<sup>C333S</sup> plasmids were cultured in 100 mL of LB medium containing 34  $\mu$ g/mL chloramphenicol, and 100  $\mu$ g/mL ampicillin at 37°C to an OD<sub>600</sub> of 0.8. The bacteria were then moved to 18°C for 30 min and the protein expression was induced by the addition of IPTG to 0.3 mM for 6 h. E. coli cells expressing Protein A-tagged Gcg1, RipAY<sup>WT</sup>, RipAY<sup>E216Q</sup> or RipAY<sup>C333S</sup> proteins were suspended in IPP150 buffer (10 mM Tris-HCl, pH 8.0, 150 mM NaCl, 50 mM EDTA) and disrupted by sonication to generate the E. coli lysates. S. cerevisiae cells carrying pMT1373-GCG1, ripAY<sup>WT</sup> or ripAY<sup>E216Q</sup> plasmids were cultured in 20 mL of SD (-Ura) liquid medium at 26°C to an OD<sub>600</sub> of 1.0 and then cells were washed twice with sterilized water and resuspended in 20 mL of SGal (-Ura) liquid medium and cultured at 26°C for 17 h to induce the protein expressions. S. cerevisiae cells expressing Protein A-tagged Gcg1, RipAY<sup>WT</sup> or RipAY<sup>E216Q</sup> proteins were suspended in 500  $\mu$ l of 1 M sorbitol-50 mM EDTA solution containing 10 mM DTT with 1 mg Zymolyase-20T (Nakarai Tesque Inc.) to obtain spheroplasts. Spheroplasts*

were washed once with 1 M sorbitol-50 mM EDTA and resuspended with 1 mL of IPP150 buffer containing 2  $\mu$ M pepstatin A and 1 mM PMSF and homogenized with a dounce homogenizer (10 strokes) on ice to generate the *S. cerevisiae* lysates. The lysates from *E. coli* or *S. cerevisiae* cells were cleared by centrifugation at 10,000  $\times$  g for 30 min at 4°C and 50  $\mu$ L of IgG-sepharose beads (50% v/v) were added into the cleared lysate and incubated for 2 h at 4°C on a rotating wheel. The beads were washed three times with the same buffer. The protein A-tagged fusion protein-immobilized beads were used for measuring the GGCT activity by a Dug1-coupled method as described above. For activation of affinity-purified Protein A-tagged RipAY from *E. coli*, the protein A-tagged fusion protein-immobilized beads were incubated with the total protein lysate from yeast cells in 1 mL IPP150 buffer at 4°C for 2 h, washed three times with IPP150 buffer and then used for measuring the GGCT activity by a Dug1-coupled method as described above.

*Immunoblot Analysis*—Yeast cells expressing GFP-tagged RipAY or other ChaC proteins were collected and resuspended in 1 mL of PBS. After the addition of trichloroacetic acid (TCA) to a final concentration of 10%, cells were incubated on ice for 15 min and precipitated by centrifugation. TCA-treated yeast cells were washed twice with 1 mL ice-cold acetone and dried. Total proteins were extracted from the dried cells by beating cells with glass beads (5 min  $\times$  2 pulses with a 5-min interval at 65°C) in Urea-SDS cracking buffer (6 M urea, 1% SDS, 50 mM Tris-HCl, pH 7.5). The total protein concentration of the cell extracts was determined using a microBCA protein assay kit (Thermo Scientific). Ten microgram aliquots of total protein were subjected to immunoblot analysis, which was performed using affinity-purified rabbit anti-GFP antiserum (our laboratory stock) or rabbit anti-G6PDH antibody (Sigma, A9521) and horseradish peroxidase-conjugated anti-rabbit IgG serum (Cell signaling technologies). Signals were detected using Immunostar LD western blotting detection reagent (Wako).

*Measurement of Total Cellular Glutathione*—Ten OD<sub>600</sub> of yeast cells expressing RipAY and their

mutants under the control of the *GALI* promoter were washed once with 1 mL of KPE (0.1 M potassium phosphate buffer with 5 mM EDTA, pH 7.5) and lysed in 200  $\mu$ L of 5% sulfosalicylic acid using glass beads. Cells were vortexed for 1 min with 1 min intervals for 10 times and centrifuged for 10 min at 4°C. Total cellular glutathione in yeast was measured as previously described (24). In brief, 10  $\mu$ L of supernatant was mixed with 60  $\mu$ L of DTNB (2 mg/3 mL) and 60  $\mu$ L of glutathione reductase (2.5 units/mL) in 96-well plate. Sixty microliters of NADPH (2 mg/3 mL) was added in the above mixtures to start the reaction. Absorbance was measured at every 15 s at 415 nm. Absorbance at 2 min was used to compare the glutathione level in the different samples. Total cellular glutathione in yeast is normalized to OD<sub>600</sub> of yeast cells.

*Measurement of Total Cellular Glutathione in Bacteria-inoculated Plants*—A 10<sup>8</sup> CFU/mL suspension of *R. solanacearum* OE1-1 (wild-type, WT) (25), RK5081 (T3SS mutant,  $\Delta$ *hrcU-1*) or RK7101 ( $\Delta$ *ripAY-4*) in an approximately 50  $\mu$ L volume was inoculated into fully expanded leaves of 6-8 week old susceptible eggplant (*Solanum melongena* cv. Senryo 2-gou) using a needleless disposable syringe, and the bacteria-inoculated plants were maintained in a greenhouse facility. Two leaf disks (0.8 cm<sup>2</sup> each) were taken 1 day after inoculation, and frozen in liquid nitrogen. The frozen samples were extracted by shaking five times with 5-mm diameter stainless beads for 30 s in a 2.0-mL screw-capped vial using a bead-beater device. Three-hundred microliters of 5% sulfosalicylic acid in KPE was added to the samples and then the samples were vortexed and centrifuged at 8,000  $\times$  g for 20 min at 4°C. Total cellular glutathione of the samples extracted from bacteria-inoculated plants was measured by the same method as that of the samples from yeast as described above. Total cellular glutathione in bacteria-inoculated leaf was normalized to mg of leaf material.

*Fluorescent Microscopic Analysis*—Fluorescence of GFP in the non-fixed yeast cells was observed using an Olympus BX51 microscope (Olympus) with a GFP filter. Images were captured with a Hamamatsu C11440-10C Orca-Flash 2.8 CMOS camera (Hamamatsu Photonics) using Metamorph

software (Molecular Device).

*Yeast Two-Hybrid Analysis*—The yeast two-hybrid (Y2H) analysis was performed using a *GAL4*-based yeast two-hybrid system according to manufacturer's instruction (MATCHMAKER Two-Hybrid System 3; Clontech). RipAY with E216Q active site mutation, RipAY<sup>E216Q</sup> was used for Y2H analysis to avoid the growth inhibition caused by its expression in yeast. The *ripAY*<sup>E216Q</sup> gene was amplified by PCR and cloned into the *EcoRI* and *BamHI* sites of pGBKT7 vector to generate a construct of RipAY<sup>E216Q</sup> fused in-frame to the Gal4 DNA-binding domain (BD) as the bait. Gateway<sup>TM</sup> technology (Life Technologies) was used to construct the prey plasmids. Thioredoxin cDNAs (*R. solanacearum* TrxA/RSc1188, *S. cerevisiae* Trx1, *Arabidopsis thaliana* Trx-h2, Trx-h3, and Trx-h5) were amplified by PCR and cloned into the gateway donor vector pDONR221 by the BP reaction. The pDONR221-Trx-h5 plasmid was used to introduce the C39, 42S active site mutation into Trx-h5. The thioredoxin genes on pDONR221 plasmid were cloned into pACT2-based gateway Gal4 activation domain (AD) plasmid, pMT731 by the LR reaction to generate the prey plasmids. The bait and prey plasmids were cotransformed into a two-hybrid reporter yeast strain AH109 cells. The transformants were spotted on SD (-Trp, -Leu) plates and SD plates with different stringency conditions (low: -Trp, -Leu, -His, medium: -Trp, -Leu, -His, + 1mM 3-AT and high: -Trp, -Leu, -His, -Ade) and the interaction of RipAY and thioredoxins was assessed by their growth under the different stringency conditions.

*Purification of the RipAY-Activator from Yeast*—Soluble proteins were extracted from 10 g of *S. cerevisiae* MTY654 (*dug3Δ ecm38Δ gcg1Δ*) cells mechanically disrupted by French Press. The extracted *S. cerevisiae* proteins were precipitated with 100% ammonium sulfate. Precipitated proteins were dialyzed overnight at 4°C against 6 L of 20 mM Tris-HCl, pH 7.5. *S. cerevisiae* proteins were separated over a HiPrep DEAE FF 16/10 ion exchange column with a salt gradient from 0 M to 1 M NaCl (GE Healthcare). Individual fractions were assayed for their ability to stimulate GGCT activity of a recombinant RipAY purified from *E. coli*. Fractions possessing

the majority of activity were pooled and dialyzed overnight at 4°C against 2 L of 20 mM Tris-HCl, pH 7.5, 1.5 M (NH<sub>4</sub>)<sub>2</sub>SO<sub>4</sub>. After dialysis, *S. cerevisiae* proteins were separated on a HiPrep Butyl FF 16/10 hydrophobic interaction column with a salt gradient from 1.5 M to 0 M (NH<sub>4</sub>)<sub>2</sub>SO<sub>4</sub> (GE Healthcare). Individual fractions retaining the activity were pooled, concentrated to 1 mL using an Amicon Ultra-2mL 3K centrifugal filter device (Millipore). Positive fractions were then separated over a HiPrep 16/60 Sephacryl 200 high resolution gel filtration column (GE Healthcare). Proteins in this final purification step contained in the positive fraction were separated by Tricine SDS-PAGE and visualized with a Sil-Best Stain One (Nakarai Tesque Inc.) or a Coomassie brilliant blue (CBB) stain.

In-gel digestion and following LC-MS/MS analysis of the activator protein from yeast was performed as described previously (26). Protein identification was performed in the Agilent Spectrum MILL MS proteomics workbench against the Swiss-Prot protein database search engine (<http://kr.expasy.org/sprot/>).

*Statistical Analysis*—Statistical analysis was performed using Graphpad Prism 6 or Microsoft Excel software, and specific tests noted in the text and figure legends.

## RESULTS

*Expression of a ChaC domain-containing effector, RipAY causes growth inhibition to yeast*—To understand the molecular mechanism of pathogenesis for *Ralstonia solanacearum*, we screened the collection of 36 previously identified effector proteins of *R. solanacearum* GM11000 (13,27) using yeast galactose inducible-expression system. This yeast expression screen revealed 8 effectors that cause growth inhibition to yeast *Saccharomyces cerevisiae*. Details of this screen along with the complete set of identified effectors will be described elsewhere (Hasegawa *et al.*, in preparation).

To predict the molecular function of identified effectors, we first searched for the functional domain or motif using the Pfam search engine (<http://pfam.xfam.org/search>) based on their primary sequences. One of the identified effectors, RipAY (locus tag RSp1022) contains a

ChaC domain, originally identified in a protein encoded by *Escherichia coli chaC*, and assumed to be a possible regulator of the *cha* operon (Ca<sup>++</sup>/H<sup>+</sup> antiporter) (28). Orthologues of the ChaC protein are found in all phyla examined. We investigated the phylogenic relationship of the protein with other ChaC protein sequences from various organisms. RipAY and Aave\_4606 identified in the genome of the cucurbit pathogenic bacterium *Acidovorax citrulli* (referred to as the class II ChaC protein family) are clearly an out-group of the ChaC proteins conserved in various organisms (referred to as the class I ChaC protein family) in a phylogenic reconstruction (Fig. 1A). Interestingly, both *R. solanacearum* and *A. citrulli* genome contain another ChaC protein, RSc0782 and Aave\_2801 respectively, which belong to the class I ChaC protein family. RipAY and Aave\_4606 have N- and C-terminal extension sequences outside of their ChaC domains and are much larger than the class I ChaC proteins (~400 a.a. for class II vs ~200 a.a. for class I) (Fig. 1B). The ChaC domain of RipAY shows lower identity to that of the class I ChaC proteins (6.2~21.3%), but higher identity to that of the class II ChaC protein, Aave\_4606 (46.4%) (Fig. 1B). It seems that RipAY and Aave\_4606 most probably originated from a duplication of the class I ChaC protein family genes and evolved to acquire a specific function as an effector.

We next examined whether heterologous expression of the other ChaC proteins also caused growth inhibition to yeast as observed in that of RipAY (Fig. 1C). Expression of neither GFP alone nor the GFP-tagged C-terminus of other ChaC proteins, showed any impact on yeast growth (Fig. 1C); nonetheless the protein expression level, except for RSc0782 and Aave\_4606, was even higher than that of RipAY in yeast (Fig. 1D). We failed to detect the expression of the Aave\_4606-GFP fusion protein in yeast, probably because the Aave\_4606 gene has a high GC content (73%) and many rare codons for yeast [34 rare codons (CGC or CGG) out of 38 total codons for arginine] (data not shown). We also examined the localization of the proteins in yeast cells using the native fluorescence of GFP fused at their C-termini and found GFP fluorescence of RipAY and most of the other ChaC proteins expressed in the cytoplasm of yeast cells (Fig. 1E and Fujiwara and Tabuchi,

unpublished result). These results suggest that RipAY affects the cytoplasmic component(s) with different activities from the other ChaC proteins.

*Expression of RipAY in yeast causes a decrease in intracellular glutathione via its GGCT activity*—Recently, it has been reported that the class I ChaC proteins from yeast, plants, and mammals function as  $\gamma$ -glutamyl cyclotransferases (GGCT) acting specifically to degrade glutathione but not other  $\gamma$ -glutamyl peptides (Fig. 2A) (18,29). The ChaC domain of RipAY has limited similarity to that of the class I ChaC proteins (Fig. 1B). However, the structure of RipAY modeled on the Phyre2 website (<http://www.sbg.bio.ic.ac.uk/phyre2/html/page.cgi?id=index>) indicated that it closely resembles the structure of human GGCT (C7orf24) (30) (Fig. 2, B and C). There is a very high structural similarity between RipAY and GGCT, although there is little amino acid similarity (data not shown). The Phyre2 search showed that most key residues in the catalytic domain of GGCT aligned with corresponding residues of RipAY (Fig. 2C). Furthermore, multiple sequence alignment of the ChaC proteins from various organisms revealed that RipAY contains the signature motifs for the substrate binding site (Y<sup>129</sup>xSL) and catalytic glutamate residue (E<sup>216</sup>) (Fig. 2D), indicating that it may function in a similar manner.

To ask directly whether RipAY had GGCT activity toward glutathione, we first determined the GGCT activity of RipAY expressed in yeast. In this regard, we employed a protein A-tag to affinity-purify the proteins using IgG-beads directly from the Protein A-tagged RipAY-expressing yeast lysates and then determined GGCT activity of the beads bound with RipAY protein using a Dug1-coupled assay for ChaC family proteins (18). To prevent contamination of endogenous glutathione degrading enzymes from the yeast lysate, we used a glutathione degrading enzyme deficient strain (*dug3Δ ecm38Δ gcg1Δ* triple mutant) to express the protein A-tagged ChaC proteins in yeast cells. Consistent with a previous report (18), the beads bound with yeast class I ChaC-family protein Gcg1 showed significant GGCT activity (Fig. 2E). Remarkably, we detected robust GGCT activity in the beads bound with wild-type RipAY (RipAY<sup>WT</sup>), but not with the catalytically inactive

mutant RipAY (RipAY<sup>E216Q</sup>). Interestingly, RipAY<sup>WT</sup> showed approximately 4.5 times higher activity than that of the beads bound with Gcg1, even though the amount of the RipAY<sup>WT</sup> protein was much lower than that of Gcg1 (Fig. 2F). This result demonstrated that RipAY protein purified from yeast possesses GGCT activity toward glutathione *in vitro*.

To ask whether yeast growth inhibition was caused by the GGCT activity of RipAY, we next performed a mutational analysis of the putative catalytic residues in the ChaC domain of RipAY and then assessed the mutants using the yeast growth inhibition test (Fig. 2G). Substitution of the putative catalytic glutamate residue to glutamine (E216Q) or the conserved substrate-binding site to alanine (Y219A, S131A, L132A) almost completely restored the yeast growth inhibition caused by expression of RipAY. However, the substitution of non-conserved leucine at position 130 (L<sup>130</sup>) to alanine (L130A) resulted in only weak restoration. Furthermore, the mutation of L<sup>130</sup> to glycine, L130G, which mimics the substrate-binding site of the class I ChaC-protein, could partially restore the growth, indicating that RipAY may have a different substrate binding mechanism from that of the class I ChaC proteins. Immunoblots were probed with anti-GFP (for RipAYs) and anti-G6PDH (as an internal control) antibodies revealing similar amounts of RipAY-GFP proteins (Fig. 2H).

We next examined whether expression of RipAY proteins affected the intracellular glutathione level in yeast (Fig. 2I). Cells over-expressing Gcg1 showed a modest decrease in glutathione (decreased to 69% relative to the control). Interestingly, cells expressing RipAY<sup>WT</sup> led to a marked decrease in glutathione (decreased to 29% relative to the control), whereas cells expressing RipAY<sup>E216Q</sup> did not show significant glutathione decrease. Together, these data showed that RipAY functions as a GGCT both *in vitro* and *in vivo*.

*Addition of exogenous glutathione did not restore the RipAY-dependent growth inhibition in yeast*—We next investigated the effect of addition of exogenous glutathione on growth of RipAY-expressing yeast cells. Unexpectedly, the addition of exogenous glutathione could not restore the RipAY-dependent growth inhibition in

both yeast WT and *gsh1Δ* mutant, which has a defect in endogenous glutathione synthesis (Fig. 3A). Interestingly, expression of the conserved substrate-binding site mutant (Y129A), whose expression does not cause growth inhibition in WT cells, causes growth inhibition in *gsh1Δ* mutant cells on medium containing 1 μM glutathione, but an excess of glutathione (100 μM) could restore this growth inhibition. Based on this result, we hypothesized that kinetics of glutathione degradation by RipAY is much faster than that of glutathione uptake by plasma membrane glutathione transporter, Hgt1 (31). As a consequence, available glutathione is limited in yeast cells expressing RipAY, causing growth inhibition. To confirm this hypothesis, we investigated the effect of over-expression of Hgt1 in yeast cells expressing RipAY. Over-expression of Hgt1 using the strong constitutive *TEF1* promoter conferred a glutathione sensitive phenotype to yeast WT cells (Fig. 3B) as previously reported (32) and showed an increased intracellular glutathione level ( $426 \pm 39\%$  for the 30 min-culture with glutathione and  $249 \pm 23\%$  for the 19 h-culture with glutathione relative to that of control cells) when cells were cultured in medium containing 100 μM glutathione (Fig. 3, C and D). Surprisingly, we observed that over-expression of Hgt1 could not restore the RipAY-dependent growth inhibition on medium containing 100 μM glutathione (Fig. 3B), even though the intracellular glutathione level was restored ( $181 \pm 10\%$  for the 30 min-culture with glutathione and  $91 \pm 15\%$  for the 19 h-culture with glutathione relative to that of control cells) in these conditions (Fig. 3, C and D). Collectively, these results indicate that RipAY has another target(s) besides glutathione at least in yeast.

*Inoculation of R. solanacearum into eggplant leaves causes a decrease in intracellular glutathione*—To explore the function of RipAY in host plant cells during *R. solanacearum* infection, we performed an inoculation test of *R. solanacearum* WT and *ripAY*-deficient ( $\Delta ripAY$ ) cells into eggplant leaf mesophyll tissues. We observed typical necrotic lesions in the area inoculated with both *R. solanacearum* WT and  $\Delta ripAY$  cells at 2 days post-inoculation, but not in the area inoculated with a type III secretion system (T3SS) mutant,  $\Delta hrcU$  and control mock (Fig. 4A),

indicating that RipAY is dispensable for virulence of *R. solanacearum* on eggplant.

We next examined glutathione levels in eggplant leaves inoculated with *R. solanacearum*. Lysates were extracted from the area inoculated with *R. solanacearum* WT,  $\Delta ripAY$ , and  $\Delta hrcU$  cells and control mock at 1 day post-inoculation, and then total glutathione level of these lysates was analyzed (Fig. 4B). We observed a modest decrease of glutathione in  $\Delta hrcU$ -inoculated eggplant leaves (decreased to 79% relative to the control), indicating pathogen associated molecular pattern (PAMP)-triggered immunity (PTI)-response may affect the host glutathione homeostasis. Strikingly, eggplant leaves inoculated with *R. solanacearum* WT showed a significant decrease in glutathione (decreased to 40% relative to the control), whereas eggplant leaves inoculated with  $\Delta ripAY$  did not show any significant decrease (Fig. 4B), implying that RipAY functions as a GGCT in host plant cells during *R. solanacearum*-infection.

*RipAY GGCT activity is triggered by a eukaryotic factor*—To perform a detailed enzyme kinetic analysis of GGCT activity of RipAY toward glutathione, recombinant RipAY and Gcg1 proteins were purified from *E. coli* using His<sub>6</sub>-tag and Ni-NTA affinity chromatography (Fig. 5A) and their GGCT activity was determined by Dug1-coupled assay (18). As shown in Fig. 5B, the recombinant Gcg1 protein showed significant GGCT activity toward glutathione as previously described (18). However, we failed to detect GGCT activity of recombinant RipAY, although we could detect robust GGCT activity in RipAY expressed in yeast (Fig. 2C). Based on these results, we hypothesized that RipAY might acquire its GGCT activity from an activator harbored in yeast cells, but not in *E. coli* cells. To test this hypothesis, the beads bound with recombinant protein A-tagged RipAY<sup>WT</sup>- or RipAY<sup>E216Q</sup> proteins expressed in *E. coli* were preincubated with a yeast extract and then GGCT activity of the beads was measured. As shown in Fig. 5C, yeast extract could stimulate the GGCT activity of RipAY<sup>WT</sup>, but not that of catalytically inactive RipAY<sup>E216Q</sup> in a dose-dependent manner, showing that yeast extract contains the activator(s) for RipAY. We did not observe any size changes in RipAY proteins after treatment with yeast



extract (Fig. 5D), indicating that activation of RipAY is not dependent on cleavage or modification of the protein. Furthermore, not only a yeast extract, but also other eukaryotic cell extracts including those of human cultured cells (HeLa), and two plants, Arabidopsis (*Arabidopsis thaliana*) and eggplant (*Solanum melongena*), but not that of *R. solanacearum*, could stimulate GGCT activity of a bacterially expressed RipAY-His<sub>6</sub> protein (Fig. 5E). These data demonstrated that RipAY acquires its GGCT activity by a eukaryote-specific factor.

*Purification and identification of the activator for RipAY from yeast extract*—Heat treatment (95°C for 5 min) or extensive dialysis of the yeast extract did not eliminate the activation of RipAY, but proteinase K treatment completely eliminated, suggesting that the activator must be heat-stable and proteinaceous (data not shown). To identify the activator of RipAY from a yeast extract, a biochemical approach was employed. Proteins extracted from yeast cells were sequentially fractionated by anion exchange, hydrophobic interaction, and gel-filtration chromatography (Fig. 6A). Fractions were assayed for their ability to stimulate GGCT activity of RipAY. Those GGCT-stimulation activities from the final purification step were analyzed by Tricine SDS-polyacrylamide gel electrophoresis (Tricine SDS-PAGE) (Fig. 6B). A single 11-kDa protein was correlated with activity (Fractions #37-41). Mass spectrometry identified this protein as Trx1 and Trx2 proteins, isoenzymes of yeast cytoplasmic thioredoxin (Trx) (Fig. 6C).

*Yeast thioredoxins can stimulate GGCT activity of RipAY both in vivo and in vitro*—The yeast proteome contains three Trx isoenzymes: two cytoplasmic isoenzymes, Trx1 and Trx2, and one mitochondrial isoenzyme, Trx3. Because RipAY is expressed in the cytoplasm in yeast cells (Fig. 1E), we expected that the growth inhibition effect caused by RipAY must be eliminated by simultaneous deletion of its candidate activators, Trx1 and Trx2. RipAY and Gcg1 proteins were expressed under the control of doxycycline repressible Tet-Off promoter (33) in yeast WT, *trx3Δ* single-, *trx1/2Δ* double- and *trx1/2/3Δ* triple-mutant cells and the growth of yeast was scored by spot assay (Fig. 7A). Interestingly, we

observed that over-expression of Gcg1 also causes growth inhibition in both *trx1/2Δ* and *trx1/2/3Δ* mutants (Fig. 7A, lower panels), suggesting that a subtle decrease of glutathione in Trx-deficient cells causes growth inhibition because Trx system shares some redundant functions in cellular redox homeostasis with the glutathione system (34). Contrary to our expectation, we still observed the growth inhibitory effect by expression of RipAY in *trx1/2Δ* mutant cells (Fig. 7A, lower middle panel). However, an additional deletion of *TRX3* from *trx1/2Δ* mutant (*trx1/2/3Δ*) clearly restores the growth inhibition (Fig. 7A, lower right panel). Consistent with these results, lysate from *trx1/2/3Δ* cells almost completely lost the activation activity of RipAY, whereas lysate from *trx1/2Δ* cells still retained weak, but significant activation activity (Fig. 7B). In addition, the lysate from *trx3Δ* cells could activate GGCT activity of RipAY and also *trx3Δ* cells expressing RipAY exhibits growth inhibition. These data indicate that major activator for RipAY in yeast cell must be Trx1 and Trx2. Finally, we demonstrated that a bacterially expressed Trx1-His<sub>6</sub> protein could stimulate GGCT activity of RipAY *in vitro* (Fig. 7C). Taken together, these results demonstrated that yeast Trxs could stimulate GGCT activity of RipAY both *in vivo* and *in vitro*.

*Plant Trxs bind to and activate RipAY in an isoform-specific manner*—Next, we investigated whether plant Trxs could also activate RipAY. Since Arabidopsis extract could activate RipAY *in vitro* (Fig. 5E) and Trxs from Arabidopsis are relatively well characterized, we employed the Arabidopsis Trxs for this purpose. The Arabidopsis genome encodes 19 Trxs belonging to six major groups, f, m, h, o, x and y (35). Whereas most of these Trxs are located in chloroplasts and mitochondria, the h-type Trxs, which consist of eight isoenzymes, are generally thought to be located in the cytoplasm. Among these h-type Trxs in Arabidopsis, *AtTrx-h2* has highest similarity to yeast Trxs (Fig. 8F). Furthermore, *AtTrx-h3* is the most highly constitutively expressed cytoplasmic Trx, and *AtTrx-h5* is substantially up-regulated upon infection with *Pseudomonas syringae* (36). We therefore chose these three Arabidopsis Trxs as candidate activators for RipAY. We first tested

whether RipAY directly interacted with Trxs using yeast two-hybrid (Y2H) analysis. As shown in Fig. 8A, we could detect the interaction of RipAY with all eukaryotic Trxs tested, but not with *R. solanacearum* Trx, *RsTrxA* under both low and medium stringency conditions (–Trp/–Leu/–His and –Trp/–Leu/–His/+3AT, respectively). However, we could detect the interaction of RipAY with only *AtTrx-h5* under high stringency conditions (–Trp/–Leu/–His/–Ade), indicating that RipAY binds *AtTrx-h5* with higher affinity than the other eukaryotic Trxs in Y2H. Trxs catalyze disulfide reduction through a redox-active site WCxPC (34). We also examined whether redox active disulfide residues of *AtTrx-h5* are required for the binding to RipAY. The redox-inactive mutant *AtTrx-h5<sup>CS</sup>*, in which active site cysteine residues at position 39 and 42 were substituted by serine, showed decreased binding and activation-activity relative to the WT, but still bound to RipAY and exhibited significant activation activity (Fig. 8, A and E). Moreover, the RipAY<sup>CS</sup> mutant, in which the sole cysteine residue at position 333 was substituted by serine, also bound to both the WT and the redox-inactive mutant of *AtTrx-h5*. Furthermore, heterologous expression of the RipAY<sup>CS</sup> mutant caused growth inhibition of yeast (Fig. 8B) and recombinant RipAY<sup>CS</sup> mutant protein expressed in *E. coli* exhibited Trx-dependent activation *in vitro*, which was similar to that of RipAY<sup>WT</sup> (Fig. 8, C and D). Taken together, these data indicate that the eukaryotic Trxs bind to RipAY without intermolecular disulfide bound-dependent covalent interaction.

We next tested if the plant Trxs stimulated GGCT activity of RipAY *in vitro*. The GGCT activity of RipAY toward glutathione was measured in the presence of various concentrations of each recombinant Trx isoenzyme. As shown in Fig. 8E, *AtTrx-h5* could most effectively stimulate GGCT activity of RipAY (more than 10-fold compared to *AtTrx-h2*:  $0.790 \pm 0.073 \mu\text{M}/\text{sec}$ , at  $5 \mu\text{M}$  *AtTrx-h5* vs  $0.066 \pm 0.009 \mu\text{M}/\text{sec}$ , at  $5 \mu\text{M}$  *AtTrx-h2*). Interestingly, the RipAY-activation activity of Trxs was correlated with the RipAY-binding ability of Trxs (Order of RipAY-activation activity: *AtTrx-h5* > *AtTrx-h3* > *ScTrx1* >> *AtTrx-h2* ≥ *AtTrx-h5<sup>CS</sup>*). Addition of *RsTrxA* to RipAY failed to stimulate GGCT activity, consistent with its inability to bind

RipAY. Taken together, these data showed that plant Trxs bind to RipAY and stimulate its GGCT activity in an isoform-specific manner.

Since heterologous expression of RipAY, but not the other ChaC proteins, caused growth inhibition to yeast (Fig. 1C) and a marked decrease of intracellular glutathione in yeast cells (Fig. 2F), we speculated that the catalytic efficiency of RipAY might be much higher than that of the class I ChaC proteins. To confirm this speculation, we performed kinetic analysis of RipAY and Gcg1 toward glutathione and compared their kinetic parameters. Both RipAY, which was activated by  $8 \mu\text{M}$  *AtTrx-h5*, and Gcg1 showed Michaelis-Menten kinetics toward glutathione (Fig. 9, A and B). We observed some inhibition at high substrate (glutathione) concentrations. The kinetic parameters revealed similar  $K_M$  values for both Gcg1 ( $1.23 \pm 0.17 \text{ mM}$ ) and RipAY ( $2.11 \pm 0.17 \text{ mM}$ ), although the  $k_{cat}$  values were markedly different, the  $k_{cat}$  value of RipAY was 160-fold higher than that of Gcg1 ( $52.8 \pm 9.58 \text{ S}^{-1}$  for RipAY vs  $0.33 \pm 0.02 \text{ S}^{-1}$  for Gcg1) (Table 1). Furthermore, the specificity constant,  $k_{cat}/K_M$  value of RipAY is 94-fold higher than that of Gcg1 ( $25.2 \pm 1.22 \text{ S}^{-1}/\text{mM}$  for RipAY vs  $0.27 \pm 0.03 \text{ S}^{-1}/\text{mM}$  for Gcg1). Collectively, we clearly demonstrated that the catalytic efficiency of RipAY is much higher than that of the class I ChaC protein.

## DISCUSSION

The T3SS effector proteins exhibit various molecular activities that generally allow bacteria to escape from host immune systems and break down barriers for pathogen growth and dissemination. Uncovering the molecular functions of T3SS effector proteins is therefore one of the most important subjects for a mechanistic understanding of pathogenesis (4). In this study, we revealed that a ChaC domain containing effector protein RipAY from the plant pathogenic bacterium *R. solanacearum* modulates the abundance of host intracellular glutathione by acting as a eukaryotic thioredoxin-dependent GGCT.

*Expression of RipAY causes growth inhibition in yeast*—We initially identified RipAY as one of the *R. solanacearum* effectors whose expression

causes growth inhibition in yeast (Fig. 1C). Subsequent analysis revealed that this growth inhibition effect might be caused by a decrease in glutathione, which is dependent on a ChaC domain in RipAY (Fig. 2E and F). Kumar *et al.* (18) reported that expression of human ChaC1 in yeast mutant cells with limited glutathione availability leads to apoptosis through depletion of intracellular glutathione and this effect is rescued by the addition of exogenous glutathione. Unexpectedly, we found that the addition of exogenous glutathione failed to rescue the growth inhibition caused by expression of RipAY (Fig. 3A). Furthermore, over-expression of Hgt1 in RipAY-expressing cells could not restore the growth inhibition on media containing glutathione, even though intracellular glutathione level was almost restored in this condition (Fig. 3, B and C). Importantly, since mutation in the putative catalytic site completely restored the growth inhibition, this effect is dependent on GGCT activity of RipAY (Fig. 3B). These data clearly indicate that yeast growth inhibition must be a consequence of RipAY-dependent degradation of another yet unidentified  $\gamma$ -glutamyl compound(s) rather than glutathione. Recently, Chi *et al.* (37) reported that mouse ChaC1/Botch, which promotes embryonic neurogenesis through inhibition of Notch signaling, deglycinates the  $\gamma$ -glutamyl-glycine at position 1,669 of Notch to prevent the S1 furin-like cleavage of Notch. Further analysis will be required for understanding the molecular mechanisms underlying the yeast growth inhibition observed in the expression of RipAY.

*RipAY is a novel type of effector that targets host glutathione*—To our knowledge, RipAY is the first T3SS effector targeting host intracellular glutathione. Glutathione has been repeatedly reported to play a crucial role in plant immune responses during biotic stresses (20). For instance, the Arabidopsis *pad2-1* mutant, which was originally identified as a phytoalexin camalexin-deficient mutant, was shown to be mutated in  $\gamma$ -glutamylcysteine synthetase (Gsh1), a critical enzyme that catalyzes the first committed step in glutathione synthesis (38). Mutant *pad2-1* plants fail to accumulate significant levels of glutathione and are rendered highly susceptible to biotrophic pathogens and insects (19). Oppositely,

enhanced level of glutathione by expression of *GSH1* in tobacco (*Nicotiana tabacum*) confers biotic stress tolerance, probably through the disease resistance-priming gene, *NPRI*-dependent salicylic acid (SA)-mediated pathway (39). Furthermore, Arabidopsis knockout mutants for one of two glutathione reductase genes, *GRI*, which show a constitutive increase in oxidized glutathione, accumulate less plant defense hormone, SA than the WT and show increased sensitivity to virulent *P. syringae* (40). We show that inoculation of *R. solanacearum* WT into eggplant leaves causes a significant decrease of glutathione and mutation of RipAY in *R. solanacearum* restores this glutathione decrease (Fig. 3B). Taken together, these results indicate that RipAY affects the host immune response by decreasing host intracellular glutathione. However, despite the importance of RipAY for host glutathione homeostasis, an *R. solanacearum* mutant lacking RipAY was not attenuated for virulence toward eggplant (Fig. 4A), arguing for the existence of additional effector proteins that interfere with a host disease-resistant signaling pathway. Indeed, a systematical effector knockout approach for *R. solanacearum* failed to identify mutants with reduced pathogenicity on two host plants, indicating a functional overlap among effectors (41).

*Regulation of the abundance of host intracellular glutathione by RipAY*—Given that most bacterial pathogens translocate only trace amounts of their effector proteins into host cell cytoplasm (42), it seemed that RipAY must be a GGCT with extremely high catalytic efficiency to decrease host intracellular glutathione during *R. solanacearum*-infection. In fact, our enzyme kinetic analysis revealed that the  $k_{cat}$  value of Trx-h5-activated RipAY was much higher than that of a *S. cerevisiae* class I ChaC-protein, Gcg1 (160-fold), although both activated RipAY and Gcg1 shows similar  $K_M$  value (Table 1). Recently, Kumar *et al.* (29) reported a detailed enzyme kinetic analysis of Arabidopsis ChaC orthologues, *AtGGCT2;2* and *AtGGCT2;3*. Based on their data, we estimated that the  $k_{cat}/K_M$  value of RipAY is 66.7- and 1081-fold higher than that of *AtGGCT2;2* and *AtGGCT2;3*, respectively (Table 1). This extremely high catalytic efficiency of thioredoxin-activated RipAY compared to the

intrinsic class I ChaC proteins is logical, as probably very limited amounts of the bacterial effector are efficiently translocated inside the plant host cells. Injection of a very active RipAY could allow depletion of the host intracellular glutathione during *R. solanacearum*-infection.

*Activation of RipAY by eukaryotic thioredoxins*—A truly unexpected finding was that for RipAY to exhibit GGCT activity, it has to be bound and activated by host plant cytoplasmic thioredoxins in an isoform-specific manner (Fig. 8E). Recent findings provide remarkable examples for the emerging concept for spatiotemporal regulation of pathogen effectors by coupling the catalytic activity to the arrival into a host cells cytoplasm (42-46). The mechanism of activation coupled with T3SS-dependent delivery ensures that eukaryotic cells are specifically and potently targeted and that the bacterium is protected from the toxic effects of its own enzymatic activity (46). Interestingly, the GGCT activity of RipAY is stimulated by thioredoxins, which are relatively well conserved within both prokaryotes and eukaryotes and the *R. solanacearum* genome also contains five thioredoxin or thioredoxin-like proteins. Our data suggest that eukaryotic, but not prokaryotic thioredoxin(s) can specifically bind to RipAY and stimulate GGCT activity of RipAY (Fig. 8, A and E). Phylogenetic tree analysis revealed that eukaryotic-type thioredoxins are clearly divided from prokaryotic-type thioredoxins (Fig. 8F). As

one might expect, our results raise two interesting questions regarding how RipAY recognizes eukaryotic thioredoxins in an isoform-specific manner and how thioredoxins stimulate the GGCT activity of RipAY. Further studies will be required for a better understanding of the mechanisms underlying thioredoxin-recognition and the enzyme activation of RipAY at the molecular level.

*A working model for the role of RipAY during R. solanacearum-infection*—Pathogen infection induces the expression of several thioredoxins in Arabidopsis (36,47). In particular, Trx-h5 plays an important role in plant defense as it was shown that Trx-h5 facilitates the reduction of NPR1 disulfides to catalyze the oligomer-to-monomer switch, which in turn promotes the activation of SA-dependent plant defense (36). Intriguingly, we found that Trx-h5 could most efficiently stimulate the GGCT activity of RipAY *in vitro* (Fig. 8E). Based on this observation, we speculate that RipAY is injected into the host plant cell via the T3SS apparatus as an inactive form and then converted to an active form by host eukaryotic thioredoxins, in particular Trx-h5 during *R. solanacearum*-infection and then degrade glutathione and other unknown  $\gamma$ -glutamyl compounds which together might prevent the activation of the host disease response (Fig. 10). Further analysis will be required for the understanding of the role of RipAY during *R. solanacearum*-infection at the molecular level.

*Acknowledgements*—We thank Tomoe Nakagawa and Jun-ichi Hasegawa for their contribution to initial experiments. We also thank Dr. Yasuomi Tada and Nodoka Oka (Nagoya University) for their valuable advice and supplying *A. thaliana* cDNA clones. We are grateful to Drs. Goro Takata and Akihide Yoshihara for their technical assistance to operate the ÄKTA Explorer system. We would like to acknowledge the technical expertise of the DNA core facility of the Gene Research Center, Kagawa University. We express our deep appreciation to Prof. Anand Bachhawat for generously providing pTEF-416-*HGT1* plasmid and for valuable discussion of the data and for critical reading of the manuscript.

*Conflict of interest*—The authors declare that they have no conflicts of interest with the contents of this article.

*Author contributions*—S.F. and M.T. designed research; S.F., K.O., T.Kitagawa, C.P., T.Kawazoe, and M.T. performed research; K.N., Y.K., M.V., S.G. contributed new reagents/analytic tools; S.F., N.T. and M.T. analyzed data; and M.T. wrote the paper. All authors analyzed the results and approved the final version of the manuscript.

## REFERENCES

1. Dean, P. (2011) Functional domains and motifs of bacterial type III effector proteins and their roles in infection. *FEMS microbiology reviews* **35**, 1100-1125
2. Bhavsar, A. P., Guttman, J. A., and Finlay, B. B. (2007) Manipulation of host-cell pathways by bacterial pathogens. *Nature* **449**, 827-834
3. Galan, J. E. (2009) Common themes in the design and function of bacterial effectors. *Cell Host Microbe*. **5**, 571-579
4. Deslandes, L., and Rivas, S. (2012) Catch me if you can: bacterial effectors and plant targets. *Trends Plant Sci.* **17**, 644-655
5. Siggers, K. A., and Lesser, C. F. (2008) The Yeast *Saccharomyces cerevisiae*: a versatile model system for the identification and characterization of bacterial virulence proteins. *Cell Host Microbe*. **4**, 8-15
6. Valdivia, R. H. (2004) Modeling the function of bacterial virulence factors in *Saccharomyces cerevisiae*. *Eukaryotic cell* **3**, 827-834
7. Lesser, C. F., and Miller, S. I. (2001) Expression of microbial virulence proteins in *Saccharomyces cerevisiae* models mammalian infection. *EMBO J.* **20**, 1840-1849
8. Salanoubat, M., Genin, S., Artiguenave, F., Gouzy, J., Mangenot, S., Arlat, M., Billault, A., Brottier, P., Camus, J. C., Cattolico, L., Chandler, M., Choisine, N., Claudel-Renard, C., Cunnac, S., Demange, N., Gaspin, C., Lavie, M., Moisan, A., Robert, C., Saurin, W., Schiex, T., Siguier, P., Thebault, P., Whalen, M., Wincker, P., Levy, M., Weissenbach, J., and Boucher, C. A. (2002) Genome sequence of the plant pathogen *Ralstonia solanacearum*. *Nature* **415**, 497-502
9. Genin, S. (2010) Molecular traits controlling host range and adaptation to plants in *Ralstonia solanacearum*. *The New phytologist* **187**, 920-928
10. Coll, N. S., and Valls, M. (2013) Current knowledge on the *Ralstonia solanacearum* type III secretion system. *Microbial biotechnology* **6**, 614-620
11. Genin, S., and Denny, T. P. (2012) Pathogenomics of the *Ralstonia solanacearum* species complex. *Annual review of phytopathology* **50**, 67-89
12. Deslandes, L., and Genin, S. (2014) Opening the *Ralstonia solanacearum* type III effector tool box: insights into host cell subversion mechanisms. *Curr. Opin. Plant Biol.* **20**, 110-117

13. Peeters, N., Carrere, S., Anisimova, M., Plener, L., Cazale, A. C., and Genin, S. (2013) Repertoire, unified nomenclature and evolution of the Type III effector gene set in the *Ralstonia solanacearum* species complex. *BMC Genomics*. **14**, 859
14. Angot, A., Peeters, N., Lechner, E., Vaillau, F., Baud, C., Gentzbittel, L., Sartorel, E., Genschik, P., Boucher, C., and Genin, S. (2006) *Ralstonia solanacearum* requires F-box-like domain-containing type III effectors to promote disease on several host plants. *Proc. Natl. Acad. Sci.* **103**, 14620-14625
15. Poueymiro, M., Cazale, A. C., Francois, J. M., Parrou, J. L., Peeters, N., and Genin, S. (2014) A *Ralstonia solanacearum* type III effector directs the production of the plant signal metabolite trehalose-6-phosphate. *mBio* **5**
16. Le Roux, C., Huet, G., Jauneau, A., Camborde, L., Tremousaygue, D., Kraut, A., Zhou, B., Levailant, M., Adachi, H., Yoshioka, H., Raffaele, S., Berthome, R., Coute, Y., Parker, J. E., and Deslandes, L. (2015) A receptor pair with an integrated decoy converts pathogen disabling of transcription factors to immunity. *Cell* **161**, 1074-1088
17. Mukaihara, T., Tamura, N., and Iwabuchi, M. (2010) Genome-wide identification of a large repertoire of *Ralstonia solanacearum* type III effector proteins by a new functional screen. *Mol. Plant Microbe. Interact.* **23**, 251-262
18. Kumar, A., Tikoo, S., Maity, S., Sengupta, S., Sengupta, S., Kaur, A., and Bachhawat, A. K. (2012) Mammalian proapoptotic factor ChaC1 and its homologues function as gamma-glutamyl cyclotransferases acting specifically on glutathione. *EMBO Rep.* **13**, 1095-1101
19. Spoel, S. H., and Loake, G. J. (2011) Redox-based protein modifications: the missing link in plant immune signalling. *Curr. Opin. Plant Biol.* **14**, 358-364
20. Dubreuil-Maurizi, C., and Poinssot, B. (2012) Role of glutathione in plant signaling under biotic stress. *Plant Signal. Behav.* **7**, 210-212
21. Ito, H., Fukuda, Y., Murata, K., and Kimura, A. (1983) Transformation of intact yeast cells treated with alkali cations. *J. Bacteriol.* **153**, 163-168
22. Imai, Y., Matsushima, Y., Sugimura, T., and Terada, M. (1991) A simple and rapid method for generating a deletion by PCR. *Nucleic Acids Res.* **19**, 2785
23. Tamura, K., Stecher, G., Peterson, D., Filipski, A., and Kumar, S. (2013) MEGA6: Molecular Evolutionary Genetics Analysis version 6.0. *Mol. Biol. Evol.* **30**, 2725-2729
24. Rahman, I., Kode, A., and Biswas, S. K. (2006) Assay for quantitative determination of

- glutathione and glutathione disulfide levels using enzymatic recycling method. *Nature Protoc.* **1**, 3159-3165
25. Kanda, A., Yasukohchi, M., Ohnishi, K., Kiba, A., Okuno, T., and Hikichi, Y. (2003) Ectopic expression of *Ralstonia solanacearum* effector protein PopA early in invasion results in loss of virulence. *Mol. Plant Microbe. Interact.* **16**, 447-455
  26. Kuramitsu, Y., Miyamoto, H., Tanaka, T., Zhang, X., Fujimoto, M., Ueda, K., Tanaka, T., Hamano, K., and Nakamura, K. (2009) Proteomic differential display analysis identified upregulated astrocytic phosphoprotein PEA-15 in human malignant pleural mesothelioma cell lines. *Proteomics* **9**, 5078-5089
  27. Poueymiro, M., and Genin, S. (2009) Secreted proteins from *Ralstonia solanacearum*: a hundred tricks to kill a plant. *Curr. Opin. Microbiol.* **12**, 44-52
  28. Ivey, D. M., Guffanti, A. A., Zemsky, J., Pinner, E., Karpel, R., Padan, E., Schuldiner, S., and Krulwich, T. A. (1993) Cloning and characterization of a putative Ca<sup>2+</sup>/H<sup>+</sup> antiporter gene from *Escherichia coli* upon functional complementation of Na<sup>+</sup>/H<sup>+</sup> antiporter-deficient strains by the overexpressed gene. *J. Biol. Chem.* **268**, 11296-11303
  29. Kumar, S., Kaur, A., Chattopadhyay, B., and Bachhawat, A. K. (2015) Defining the Cytosolic Pathway of Glutathione Degradation in *Arabidopsis thaliana*: Role of the ChaC/GCG Family of gamma-glutamyl cyclotransferases as Glutathione Degrading Enzymes and AtLAP1 as the Cys-Gly Peptidase. *Biochem. J.* **468**, 73-85
  30. Oakley, A. J., Yamada, T., Liu, D., Coggan, M., Clark, A. G., and Board, P. G. (2008) The identification and structural characterization of C7orf24 as gamma-glutamyl cyclotransferase. An essential enzyme in the gamma-glutamyl cycle. *J. Biol. Chem.* **283**, 22031-22042
  31. Bourbouloux, A., Shahi, P., Chakladar, A., Delrot, S., and Bachhawat, A. K. (2000) Hgt1p, a high affinity glutathione transporter from the yeast *Saccharomyces cerevisiae*. *J. Biol. Chem.* **275**, 13259-13265
  32. Kumar, C., Igbaria, A., D'Autreaux, B., Planson, A. G., Junot, C., Godat, E., Bachhawat, A. K., Delaunay-Moisan, A., and Toledano, M. B. (2011) Glutathione revisited: a vital function in iron metabolism and ancillary role in thiol-redox control. *EMBO J.* **30**, 2044-2056
  33. Tabuchi, M., Kawai, Y., Nishie-Fujita, M., Akada, R., Izumi, T., Yanatori, I., Miyashita, N., Ouchi, K., and Kishi, F. (2009) Development of a novel functional high-throughput

- screening system for pathogen effectors in the yeast *Saccharomyces cerevisiae*. *Biosci. Biotechnol. Biochem.* **73**, 2261-2267
34. Meyer, Y., Buchanan, B. B., Vignols, F., and Reichheld, J. P. (2009) Thioredoxins and glutaredoxins: unifying elements in redox biology. *Annu. Rev. Genet.* **43**, 335-367
  35. Gelhaye, E., Rouhier, N., Navrot, N., and Jacquot, J. P. (2005) The plant thioredoxin system. *Cell. Mol. Life Sci.* **62**, 24-35
  36. Tada, Y., Spoel, S. H., Pajerowska-Mukhtar, K., Mou, Z., Song, J., Wang, C., Zuo, J., and Dong, X. (2008) Plant immunity requires conformational changes [corrected] of NPR1 via S-nitrosylation and thioredoxins. *Science* **321**, 952-956
  37. Chi, Z., Byrne, S. T., Dolinko, A., Harraz, M. M., Kim, M. S., Umanah, G., Zhong, J., Chen, R., Zhang, J., Xu, J., Chen, L., Pandey, A., Dawson, T. M., and Dawson, V. L. (2014) Botch is a gamma-glutamyl cyclotransferase that deglycinates and antagonizes Notch. *Cell Rep.* **7**, 681-688
  38. Parisy, V., Poinssot, B., Owsianowski, L., Buchala, A., Glazebrook, J., and Mauch, F. (2007) Identification of PAD2 as a gamma-glutamylcysteine synthetase highlights the importance of glutathione in disease resistance of Arabidopsis. *Plant J.* **49**, 159-172
  39. Ghanta, S., Bhattacharyya, D., Sinha, R., Banerjee, A., and Chattopadhyay, S. (2011) *Nicotiana tabacum* overexpressing gamma-ECS exhibits biotic stress tolerance likely through NPR1-dependent salicylic acid-mediated pathway. *Planta* **233**, 895-910
  40. Mhamdi, A., Hager, J., Chaouch, S., Queval, G., Han, Y., Tacconnat, L., Saindrenan, P., Gouia, H., Issakidis-Bourguet, E., Renou, J. P., and Noctor, G. (2010) Arabidopsis GLUTATHIONE REDUCTASE1 plays a crucial role in leaf responses to intracellular hydrogen peroxide and in ensuring appropriate gene expression through both salicylic acid and jasmonic acid signaling pathways. *Plant Physiol.* **153**, 1144-1160
  41. Cunnac, S., Occhialini, A., Barberis, P., Boucher, C., and Genin, S. (2004) Inventory and functional analysis of the large Hrp regulon in *Ralstonia solanacearum*: identification of novel effector proteins translocated to plant host cells through the type III secretion system. *Mol. Microbiol.* **53**, 115-128
  42. Gaspar, A. H., and Machner, M. P. (2014) VipD is a Rab5-activated phospholipase A1 that protects *Legionella pneumophila* from endosomal fusion. *Proc. Natl. Acad. Sci.* **111**, 4560-4565
  43. Fu, H., Coburn, J., and Collier, R. J. (1993) The eukaryotic host factor that activates



exoenzyme S of *Pseudomonas aeruginosa* is a member of the 14-3-3 protein family. *Proc. Natl. Acad. Sci.* **90**, 2320-2324

44. Christen, M., Coye, L. H., Hontz, J. S., LaRock, D. L., Pfuetzner, R. A., Megha, and Miller, S. I. (2009) Activation of a bacterial virulence protein by the GTPase RhoA. *Sci. Signal.* **2**, ra71
45. Coaker, G., Falick, A., and Staskawicz, B. (2005) Activation of a phytopathogenic bacterial effector protein by a eukaryotic cyclophilin. *Science* **308**, 548-550
46. Anderson, D. M., Schmalzer, K. M., Sato, H., Casey, M., Terhune, S. S., Haas, A. L., Feix, J. B., and Frank, D. W. (2011) Ubiquitin and ubiquitin-modified proteins activate the *Pseudomonas aeruginosa* T3SS cytotoxin, ExoU. *Mol. Microbiol.* **82**, 1454-1467
47. Laloi, C., Mestres-Ortega, D., Marco, Y., Meyer, Y., and Reichheld, J. P. (2004) The *Arabidopsis* cytosolic thioredoxin h5 gene induction by oxidative stress and its W-box-mediated response to pathogen elicitor. *Plant Physiol.* **134**, 1006-1016

## FOOTNOTES

This work was supported by JSPS KAKENHI Grants Numbers 22580095 and 25450104 and also, in part, by the General Research Grant of Institute of Fermentation, Osaka (IFO).

The abbreviations used are as follows: GFP, green fluorescent protein; IPTG, isopropyl-1-thio-β-D-galactopyranoside; mAb, monoclonal antibody; pAb, polyclonal antibody; WT, wild-type; GSH, reduced glutathione; GSSG, oxidized glutathione; GGCT, γ-glutamyl cyclotransferase; GGT, γ-glutamyltranspeptidase; T3SS, Type III secretion system; G6PDH, glucose 6-phosphate dehydrogenase

## FIGURE LEGENDS

**FIGURE 1. Expression of RipAY, but not other ChaC family proteins from various organisms, causes growth inhibition to yeast.** (A) Phylogenetic analysis of ChaC domain containing proteins from various organisms. The organisms, locus tag/gene name, and (Genbank<sup>TM</sup> Accession numbers) are as follows: *Escherichia coli* ChaC (L28709.1); *Ralstonia solanacearum* RSc0782(AL646052.1) and RSp1022/RipAY (AL646053.1); *Acidovorax citrulli* Aave\_2801 (CP000512.1) and Aave\_4606 (CP000512.1); *Pseudomonas syringae* PSPT\_05239 (AE016853.1); *Saccharomyces cerevisiae* YER163c/Gcg1 (NM\_001179053.3); *Aspergillus oryzae* ChaC (XM\_001818295.2); *Homo sapiens* ChaC1 (NM\_001142776.1) and ChaC2 (NM\_001008708.2); *Mus musculus* ChaC1 (NM\_026929.4) and ChaC2 (NM\_026527.3); *Xenopus tropicalis* ChaC1 (NM\_001130284.1) and ChaC2 (NM\_001017137.2); *Gallus gallus* ChaC1 (NM\_001199656.1) and ChaC2 (AJ720918.1); *Danio rerio* ChaC1 (NM\_001110126.1) and ChaC2 (BC154137.1); *Arabidopsis thaliana* AT5G26220/GGCT2;1 (BT005234.1), AT4G31290/GGCT2;2 (BT006411.1) and AT1G44790/GGCT2;3 (BT006192.1) (B) Schematic representation of putative domain organization of ChaC domain containing proteins from various organisms. (C) Yeast growth inhibition assay showing serial dilutions of *S. cerevisiae* BY4743 cells grown under inducing (galactose) or noninducing (glucose) conditions that are carrying plasmids expressing the C-terminal GFP-tagged indicated proteins under the control of *GALI* promoter. The cells were grown at 26°C for 2 days for SD (-Ura) and 3 days for SGal (-Ura). (D, E) Detections of the ChaC domain-containing proteins expressed in yeast. Yeast cells carrying the plasmids expressing GFP-tagged RipAY or other ChaC-proteins under the control of *GALI* promoter were grown in SD (-Ura) liquid medium to mid-log phase, then shifted to SGal (-Ura) liquid medium to induce the protein expression, further cultured for 12 h, and analyzed by (D) immunoblot with anti-GFP antibody or (E) fluorescence microscopy with native GFP fluorescence. Glucose 6-phosphate dehydrogenase (G6PDH) was used as a loading control. Scale bar = 5 μm

**FIGURE 2. Expression of RipAY in yeast causes growth inhibition by depletion of intracellular glutathione through its conserved ChaC domain.** (A) The GSH catabolism by a classical GGT- and GGCT-dependent and a novel ChaC family-dependent pathways, GGT:  $\gamma$ -glutamyl tranpeptidase, GGCT:  $\gamma$ -glutamyl cyclotransferase (B) The RipAY protein was modeled using the Phyre2 server. The homology model obtained was superimposed on the crystal structure of GGCT (C7orf24, PDB code 2PN7 and 2RBH) using the graphics program CueMol. Superimposition of homology-modeled RipAY structure (green color) on GGCT structure (blue color). (C) Putative active site residues of RipAY (Y<sup>129</sup>LSL and E<sup>216</sup>, green color) were superimposed on corresponding active site residues of GGCT (Y<sup>22</sup>GSN and E<sup>98</sup>, blue color). (D) Multiple alignment of amino acid sequences in the regions of putative substrate binding- and catalytic-sites of the class I and II ChaC proteins. The conserved amino acids, Y<sup>129</sup>xSL and E<sup>216</sup> are putative substrate binding-site and catalytic glutamate residue for GGCT, respectively. (E) Protein A-tagged Gcg1, RipAY WT and active site mutant, E216Q were expressed in a glutathione degrading enzyme deficient strain (*dug3Δ ecm38Δ gcg1Δ* triple mutant) of yeast cells and immunopurified with IgG-beads. The GGCT activity of the beads immobilized with Gcg1, RipAY<sup>WT</sup> or RipAY<sup>E216Q</sup> proteins, was measure by Dug1-coupled method as described in Experimental Procedures. (F) The proteins extracted from the beads shown in (E) were resolved on SDS-PAGE followed by immunoblotting using a rabbit IgG. (G) Mutations in putative substrate binding- and catalytic-sites of RipAY restore the yeast growth inhibition caused by expression of RipAY. Yeast cells carrying empty vector or *GALI*-expression vector of WT or indicated mutant proteins of RipAY were spotted on SD (-Ura) and SGal (-Ura) plates and cultured for 2 days and 3 days, respectively. (H) Yeast cells carrying *GALI*-expression plasmid of GFP-tagged WT or indicated mutant proteins of RipAY were grown in SD (-Ura) liquid medium to mid-log phase and then shifted to SGal (-Ura) liquid medium to induce the protein expression, further cultured for 12 h, and analyzed by immunoblot with anti-GFP antibody. (I) Mutations in putative substrate binding- and catalytic-sites of RipAY restore the reduction of intracellular GSH level in yeast caused by expression of RipAY. The total GSH levels of the cell lysates from yeast cells expressing

indicated proteins were measured as described in Experimental Procedures. Values represent the mean  $\pm$  SEM ( $n \geq 3$ ).

**FIGURE 3. Increased uptake of GSH does not rescue the growth inhibition effect caused by expression of RipAY.** (A) Yeast wild-type and *gsh1Δ/gsh1Δ* homozygote cells carrying indicated plasmids were spotted on SD (-ura) (OFF) or SGal (-leu, -ura) (ON) plates supplemented with the indicated concentration of GSH. Cells were incubated at 26°C for 2 days for SD (-leu, -ura) or 3 days for SGal (-leu, -ura). (B) Yeast cells carrying indicated plasmids were spotted on SD (-leu, -ura) (RipAY-expression: OFF) or SGal (-leu, -ura) (RipAY-expression: ON) plates supplemented with the indicated concentration of GSH. Cells were incubated at 26°C for 2 days for SD (-leu, -ura) or 3 days for SGal (-leu, -ura). RipAY or *HGT1* were expressed under the control of a galactose-inducible *GAL1* promoter or a strong constitutive *TEF1* promoter, respectively. (C) Yeast cells carrying indicated plasmids growing exponentially in SD (-leu, -ura) liquid medium were transferred to SGal (-leu, -ura) liquid medium and cultured at 26°C for 19 h and then GSH (100 μM) was supplemented at 30 min prior to the termination of the culture. (D) Yeast cells carrying indicated plasmids growing exponentially in SD (-leu, -ura) liquid medium were transferred to SGal (-leu, -ura) liquid medium supplemented with or without 100 μM GSH and cultured at 26°C for 19 h. The total GSH levels of the cell lysates from yeast cells expressing indicated proteins were measured. Values represent the mean  $\pm$  SEM ( $n=4$  for C and  $n=3$  for D).

**FIGURE 4. The GSH level of eggplant leaves inoculated with *R. solanacearum* wild-type, RipAY- and T3SS-deficient strains.** (A) Necrotic lesions on eggplant leaf three days post-inoculation with *R. solanacearum* WT strain (WT), RipAY deficient strain ( $\Delta$ *ripAY*), or T3SS deficient strain ( $\Delta$ *hrcU*). Mock indicates inoculation of buffer without bacteria as a control. (B) The GSH level of total lysate extracted from eggplant leaves inoculated with the indicated *R. solanacearum* strains at one day post-inoculation was measured as described in Experimental Procedures. Values represent the mean  $\pm$  SEM ( $n \geq 7$ ). \*\* $P < 0.01$ , \*\*\* $P < 0.001$ , one-way ANOVA post test (Turkey's multiple comparison test).

**FIGURE 5. RipAY exhibits GGCT activity in the presence of eukaryotic factor(s).**

(A) Purification of recombinant Gcg1 and RipAY proteins. Recombinant His<sub>6</sub>-tagged Gcg1 and RipAY were expressed in *E. coli* and purified using Ni-NTA affinity chromatography. Purified proteins were analyzed on SDS-PAGE with Coomassie blue staining. (B) Measurement of GGCT activity of recombinant Gcg1 and RipAY purified from *E. coli*. 0.1 μg of Gcg1 and 1 μg of RipAY were incubated with 5 mM glutathione, the reactions were terminated at indicated time points, the released Cys-Gly dipeptides were digested with Cys-Gly dipeptidase Dug1 and then the released Cys was measured by acidic ninhydrin. (C) Effect of concentration of the yeast protein extract on activation of GGCT activity of RipAY. The beads bound with RipAY<sup>WT</sup> or RipAY<sup>E216Q</sup> proteins expressed in *E. coli* were pre-incubated with different concentrations of native yeast protein extracted from a glutathione degrading enzyme deficient strain (*dug3Δ ecm38Δ gcg1Δ* triple mutant) for 2 h at 4°C and washed with the same buffer three times and then GGCT activity of the beads was measured by the Dug1-coupled method. (D) The protein A-tagged RipAY<sup>WT</sup> and RipAY<sup>E216Q</sup> proteins extracted from the beads shown in (C) were resolved on SDS-PAGE and visualized by CBB staining. (E) The GGCT activity of bacterially expressed RipAY-His<sub>6</sub> protein incubated with 10 μg protein of the cell lysates from *R. solanacearum*, *S. cerevisiae*, human cultured cell HeLa, *A. thaliana*, or egg plant *S. melongena* cells was measured by Dug1-coupled method. Values represent the mean  $\pm$  SEM ( $n \geq 3$ ).

**FIGURE 6. Identification of thioredoxin as a eukaryotic activator for GGCT activity of RipAY.** (A) Biochemical purification of RipAY's eukaryotic activator from yeast protein extracts by HiPrep DEAE FF 16/10 ion exchange, HiPrep Butyl FF 16/10 hydrophobic interaction, and HiPrep 16/60 Sephacryl S-100 HR gel filtration chromatography. (B) Gel-filtration fractions surrounding activity were loaded onto a Tricine-SDS-PAGE gel, visualized by silver-staining. (C) Gel bands of fractions 37-41 stained with

Coomassie brilliant blue were collected and in-gel digestion and following LC-MS/MS analysis identified yeast thioredoxins, Trx1 and Trx2 proteins as the activator. Amino acid sequences of *S. cerevisiae* Trx1 and Trx2 and their corresponding tryptic peptides identified by LC-MS/MS analysis were shown.

**FIGURE 7. Yeast thioredoxins can activate a GGCT activity of RipAY both *in vivo* and *in vitro*.** (A) *S. cerevisiae* WT, *trx3Δ* single mutant, *trx1/2Δ* double mutant and *trx1/2/3Δ* triple mutant cells carrying plasmid expressing RipAY or Gcg1 under the control of *Tet-off* promoter were grown in noninducing (+Dox) or inducing (-Dox) conditions. Yeast cells transformed with corresponding empty vector was used as a control. The cells were grown at 26°C for 3 days for SD (-Ura, +Dox) and 4 days for SD (-Ura, -Dox). (B) The GGCT activity of bacterially expressed RipAY-His<sub>6</sub> protein incubated with 10 μg protein of the cell lysates from indicated *S. cerevisiae* thioredoxin mutant cells was measured by the Dug1-coupled method. Values represent the mean ± SEM (n≥3). (C) Bacterially expressed *S. cerevisiae* Trx1-His<sub>6</sub> protein can activate the GGCT activity of bacterially expressed RipAY-His<sub>6</sub> protein.

**FIGURE 8. Plant thioredoxins can bind to RipAY and activate GGCT activity of RipAY in an isoform-specific manner.** (A) Yeast two-hybrid assay for interaction between RipAY and various thioredoxins on the plate with different stringency conditions. RipAY WT (RipAY<sup>WT</sup>) and mutant form of RipAY (RipAY<sup>CS</sup>), in which the sole cysteine residue at position 333 was substituted by serine, were used as bait. *R. solanacearum* TrxA (*RsTrxA*), *S. cerevisiae* Trx1 (*ScTrx1*), *A. thaliana* Trx-h2, -h3, -h5 (*AtTrx-h2*, *AtTrx-h3*, and *AtTrx-h5*) and mutant form of Trx-h5 (*AtTrx-h5<sup>CS</sup>*), in which active site cysteine residues at position 39 and 42 were substituted by serine, were used as prey. (B) Yeast cells carrying empty vector or *GALI*-expression vector of WT, active site mutant E216Q or C333S mutant of RipAY were spotted on SD (-Ura) and SGal (-Ura) plates and cultured for 2 days and 3 days, respectively. (C) GGCT activity of the beads bound with protein A-tagged RipAY<sup>WT</sup>, RipAY<sup>E216Q</sup> or RipAY<sup>C333S</sup> proteins expressed in *E. coli* incubated with 1.6 μM *AtTrx-h5*-His<sub>6</sub> protein was measured by the Dug1-coupled method. Values represent the mean ± SEM (n=3). (D) Protein A-tagged RipAY<sup>WT</sup>, RipAY<sup>E216Q</sup> and RipAY<sup>C333S</sup> proteins extracted from the beads shown in (C) were resolved on SDS-PAGE and visualized by CBB staining. (E) Effect of thioredoxin isoforms on activation of GGCT activity of RipAY. The GGCT activity of RipAY incubated with various concentrations of thioredoxin isoforms was measured by the Dug1-coupled method. Values represent the mean ± SEM (n≥3). (F) Phylogenetic analysis of thioredoxin isoforms from various organisms. The organisms, locus tag/gene name, and (Genbank<sup>TM</sup> Accession numbers) are as follows: *R. solanacearum*, RSc1188/*RsTrxA* (AL646052.1) and RSc0779/*RsTrx* (AL646052.1); *E. coli*, *EcTrxA* (M26133.1) and *EcTrxC* (U8594.1); *H. sapiens*, *HsTxn1* (JQ313905.1) and *HsTxn2* (DQ891579.2); *S. cerevisiae*, YLR043C/*ScTrx1* (NM\_001181930.1), YGR209C/*ScTrx2* (NM\_001181338.3) and YCR083C/*ScTrx3* (NM\_001178789.1); *A. thaliana*, At3g51030/*AtTrx-h1* (NM\_114963.4), At5g39950/*AtTrx-h2* (AY113052.1), At5g42980/*AtTrx-h3* (AY065098.1), At1g19730/*AtTrx-h4* (BT004710.1), At1g45145/*AtTrx-h5* (AY040028.1), At1g59730/*AtTrx-h7* (BT0031540.1), At1g69880/*AtTrx-h8* (BT003670.1) and At3g08710/*AtTrx-h9* (BT0011728.1)

**FIGURE 9. Enzyme kinetic analysis of activated RipAY and Gcg1.** (A) Michaelis-Menten plot of Trx-h5-activated RipAY and (B) Gcg1 toward glutathione. Gcg1 (0.8 μM) or RipAY (0.04 μM) in the presence of Trx-h5 (8 μM) was used for determination of kinetic parameters. Different concentration of glutathione were used ranging from 0.5 mM to 20 mM. Dug1-coupled assay was used for the study as described in experimental procedures. Data of three independent experiments were analyzed by non-linear regression using GraphPad prism 6.0.

**FIGURE 10. A model depicting how the RipAY T3SS effector is activated by host eukaryotic-thioredoxins to trigger GGCT activity.** RipAY is injected into a host plant cell as an inactive form and then stimulated its GGCT activity by host eukaryotic thioredoxins, such as Trx-h5 to degrade glutathione and other unknown  $\gamma$ -glutamyl compound(s).

**TABLE 1 Strains used in this study**

Strain	Genotype	Reference or source
<i>Saccharomyces cerevisiae</i>		
BY4741	<i>MATa his3Δ1 leu2Δ0 met15Δ0 ura3Δ0</i>	Research Genetics
BY4742	<i>MATα his3Δ1 leu2Δ0 lys2Δ0 ura3Δ0</i>	Research Genetics
BY4743	BY4741/BY4742	Research Genetics
MTY654	BY4741 <i>dug3Δ::KanMX4 ecm38Δ::KanMX4 gcg1Δ::KanMX4</i>	This study
MTY674	BY4741 <i>trx1Δ::KanMX4</i>	This study
MTY676	BY4741 <i>trx2Δ::KanMX4</i>	This study
MTY678	BY4741 <i>trx3Δ::KanMX4</i>	This study
MTY680	BY4741 <i>trx1Δ::KanMX4 trx2Δ::KanMX4</i>	This study
MTY761	BY4741 <i>trx1Δ::KanMX4 trx2Δ::KanMX4 trx3Δ::KanMX4</i>	This study
<i>gsh1Δ/gsh1Δ</i>	BY4743 <i>gsh1Δ::KanMX4 / gsh1Δ::KanMX4</i>	Research Genetics
AH109	<i>MATa trp1-901 leu2-3 112 ura3-52 his3-200 gal4Δ gal80Δ</i> <i>LYS2::GAL1<sub>UAS</sub>-GAL1<sub>TATA</sub>-HIS3 MEL1 GAL2<sub>UAS</sub>-GAL2<sub>TATA</sub>-ADE2</i> <i>URA3::MEL1<sub>UAS</sub>-MEL1<sub>TATA</sub>-LacZ</i>	Clontech
<i>Ralstonia solanacearum</i>		
OE1-1	wild-type, pathogenic to tobacco, eggplant isolate	25
RK5081	OE1-1 <i>ΔhrcU-1</i>	This study
RK7101	OE1-1 <i>ΔripAY-4</i>	This study

**TABLE 2. *S. cerevisiae* plasmids used in this study**

Plasmids	Construct	Reference or source
pMT751	<i>URA3</i> , 2 $\mu$ , <i>P<sub>GALI</sub></i> - <i>attR1-Cm<sup>r</sup>-ccdB-attR2</i> -GFP	33
pMT830	<i>URA3</i> , 2 $\mu$ , <i>P<sub>tet-off</sub></i> - <i>attR1-Cm<sup>r</sup>-ccdB-attR2</i> -GFP	33
pMT1373	<i>URA3</i> , 2 $\mu$ , <i>P<sub>GALI</sub></i> - <i>attR1-Cm<sup>r</sup>-ccdB-attR2</i> -Protein A	This study
pGBKT7	<i>TRP1</i> , 2 $\mu$ , Yeast two hybrid <i>GAL4</i> DNA-BD vector	Clontech
pGADT7	<i>LEU2</i> , 2 $\mu$ , Yeast two hybrid <i>GAL4</i> AD vector	Clontech
pACT2	<i>LEU2</i> , 2 $\mu$ , Yeast two hybrid <i>GAL4</i> AD vector	Clontech
pMT731	pACT2; <i>GAL4</i> AD- <i>attR1-Cm<sup>r</sup>-ccdB-attR2</i>	This study
pMT922	pMT830; <i>URA3</i> , 2 $\mu$ , <i>P<sub>tet-off</sub></i> -GFP	33
pRE85	pMT751; <i>URA3</i> , 2 $\mu$ , <i>P<sub>GALI</sub></i> - <i>R. solanacearum RipAY</i> -GFP	This study
pRE97	pMT751; <i>URA3</i> , 2 $\mu$ , <i>P<sub>GALI</sub></i> - <i>R. solanacearum RSc0782</i> -GFP	This study
pRE98	pMT751; <i>URA3</i> , 2 $\mu$ , <i>P<sub>GALI</sub></i> - <i>H. sapiens Chac2</i> -GFP	This study
pRE99	pMT751; <i>URA3</i> , 2 $\mu$ , <i>P<sub>GALI</sub></i> - <i>P. syringae PSPTO_5239</i> -GFP	This study
pRE100	pMT751; <i>URA3</i> , 2 $\mu$ , <i>P<sub>GALI</sub></i> - <i>S. cerevisiae GCG1</i> -GFP	This study
pRE161	pMT751; <i>URA3</i> , 2 $\mu$ , <i>P<sub>GALI</sub></i> - <i>A. citrulli Aave_4606</i> -GFP	This study
pRE173	pMT751; <i>URA3</i> , 2 $\mu$ , <i>P<sub>GALI</sub></i> - <i>A. thaliana AT1G44790/GGCT2;3</i> -GFP	This study
pRE174	pMT751; <i>URA3</i> , 2 $\mu$ , <i>P<sub>GALI</sub></i> - <i>A. thaliana AT4G31290/GGCT2;2</i> -GFP	This study
pRE175	pMT751; <i>URA3</i> , 2 $\mu$ , <i>P<sub>GALI</sub></i> - <i>A. thaliana AT5G26220/GGCT2;1</i> -GFP	This study
pRE86	pMT751; <i>URA3</i> , 2 $\mu$ , <i>P<sub>GALI</sub></i> - <i>RipAY<sup>E216Q</sup></i> -GFP	This study
pRE164	pMT751; <i>URA3</i> , 2 $\mu$ , <i>P<sub>GALI</sub></i> - <i>RipAY<sup>2Y129A</sup></i> -GFP	This study
pRE165	pMT751; <i>URA3</i> , 2 $\mu$ , <i>P<sub>GALI</sub></i> - <i>RipAY<sup>L130A</sup></i> -GFP	This study
pRE166	pMT751; <i>URA3</i> , 2 $\mu$ , <i>P<sub>GALI</sub></i> - <i>RipAY<sup>S131A</sup></i> -GFP	This study
pRE167	pMT751; <i>URA3</i> , 2 $\mu$ , <i>P<sub>GALI</sub></i> - <i>RipAY<sup>L132A</sup></i> -GFP	This study
pRE168	pMT751; <i>URA3</i> , 2 $\mu$ , <i>P<sub>GALI</sub></i> - <i>RipAY<sup>L130G</sup></i> -GFP	This study
pSF38	pMT751; <i>URA3</i> , 2 $\mu$ , <i>P<sub>GALI</sub></i> - <i>RipAY<sup>C333S</sup></i> -GFP	This study
pRE257	pMT1373; <i>URA3</i> , 2 $\mu$ , <i>P<sub>GALI</sub></i> - <i>S. cerevisiae GCG1</i> -Protein A	This study
pRE258	pMT1373; <i>URA3</i> , 2 $\mu$ , <i>P<sub>GALI</sub></i> - <i>RipAY</i> -Protein A	This study
pRE259	pMT1373; <i>URA3</i> , 2 $\mu$ , <i>P<sub>GALI</sub></i> - <i>RipAY<sup>E216Q</sup></i> -Protein A	This study
pSF25	pGBKT7; <i>TRP1</i> , 2 $\mu$ , <i>P<sub>ADHI</sub></i> - <i>GAL4</i> DNA-BD- <i>RipAY<sup>E216Q</sup></i>	This study
pSF37	pGBKT7; <i>TRP1</i> , 2 $\mu$ , <i>P<sub>ADHI</sub></i> - <i>GAL4</i> DNA-BD- <i>RipAY<sup>E216Q, C333S</sup></i>	This study
pRE249	pGADT7; <i>LEU2</i> , 2 $\mu$ , <i>P<sub>ADHI</sub></i> - <i>GAL4</i> AD- <i>A. thaliana TRX h2</i>	This study
pRE250	pGADT7; <i>LEU2</i> , 2 $\mu$ , <i>P<sub>ADHI</sub></i> - <i>GAL4</i> AD- <i>A. thaliana TRX h3</i>	This study
pSF50	pMT731; <i>LEU2</i> , 2 $\mu$ , <i>P<sub>ADHI</sub></i> - <i>GAL4</i> AD- <i>A. thaliana TRX h5</i>	This study
pSF51	pMT731; <i>LEU2</i> , 2 $\mu$ , <i>P<sub>ADHI</sub></i> - <i>GAL4</i> AD- <i>A. thaliana TRX h5<sup>C39, 42S</sup></i>	This study
pSF52	pMT731; <i>LEU2</i> , 2 $\mu$ , <i>P<sub>ADHI</sub></i> - <i>GAL4</i> AD- <i>S. cerevisiae TRX1</i>	This study
pMT1416	pMT731; <i>LEU2</i> , 2 $\mu$ , <i>P<sub>ADHI</sub></i> - <i>GAL4</i> AD- <i>R. solanacearum TrxA</i>	This study
pTEF1-416- <i>HGT1</i>	pRS416; <i>URA3</i> , <i>CEN</i> , <i>P<sub>TEF1</sub></i> - <i>S. cerevisiae HGT1</i>	31

**TABLE 3. *E. coli* plasmids used in this study**

Plasmids	Construct	Reference or source
pET23d	<i>Amp</i> , $P_{T7}$ , the C-terminal His <sub>6</sub> -tag fusion vector	Novagen, Inc
pDEST17	<i>Amp</i> , $P_{T7}$ , the Gateway N-terminal His <sub>6</sub> -tag fusion vector	Life Technologies
pMT1371	pET23d: $P_{T7}$ - <i>attR1-Cm<sup>r</sup>-ccdB-attR2-Protein A</i>	This study
pSF16	pET23d: $P_{T7}$ - <i>R. solanacearum RipAY-His<sub>6</sub></i>	This study
pSF17	pET23d: $P_{T7}$ - <i>S. cerevisiae GCG1-His<sub>6</sub></i>	This study
pSF16	pET23d: $P_{T7}$ - <i>R. solanacearum RipAY-His<sub>6</sub></i>	This study
pSF40	pET23d: $P_{T7}$ - <i>S. cerevisiae TRX1-His<sub>6</sub></i>	This study
pSF49	pDEST17: $P_{T7}$ -Met-His <sub>6</sub> - <i>A. thaliana TRX h5</i>	This study
pMT1293	pET23d: $P_{T7}$ - <i>S. cerevisiae DUG1-His<sub>6</sub></i>	This study
pMT1409	pDEST17: $P_{T7}$ -Met-His <sub>6</sub> - <i>A. thaliana TRX h2</i>	This study
pMT1410	pDEST17: $P_{T7}$ -Met-His <sub>6</sub> - <i>A. thaliana TRX h3</i>	This study
pMT1411	pDEST17: $P_{T7}$ -Met-His <sub>6</sub> - <i>A. thaliana TRX h5<sup>C39, 42S</sup></i>	This study
pMT1415	pDEST17: $P_{T7}$ -Met-His <sub>6</sub> - <i>R. solanacearum TrxA</i>	This study
pMT1368	pMT1371: $P_{T7}$ -ProteinA	This study
pRE254	pMT1371: $P_{T7}$ - <i>S. crevisiae GCG1-ProteinA</i>	This study
pRE255	pMT1371: $P_{T7}$ - <i>R. solanacearum RipAY-ProteinA</i>	This study
pRE256	pMT1371: $P_{T7}$ - <i>R. solanacearum RipAY<sup>E216Q</sup>-ProteinA</i>	This study
pRE496	pMT1371: $P_{T7}$ - <i>R. solanacearum RipAY<sup>C333S</sup>-ProteinA</i>	This study

**TABLE 4 Kinetic Parameters of *S. cerevisiae* Gcg1 and *Af*Trx-h5-activated RipAY**

Enzyme	$K_M$ (mM)	$k_{cat}$ (s <sup>-1</sup> )	$k_{cat}/K_M$ (s <sup>-1</sup> mM <sup>-1</sup> )	Comparison of $k_{cat}/K_M$ value v.s. RipAY		
				Gcg1	<i>At</i> GGCT2;2**	<i>At</i> GGCT2;3**
Gcg1	1.23 ± 0.17	0.33 ± 0.02	0.27 ± 0.03			
RipAY*	2.11 ± 0.17	52.8 ± 9.58	25.2 ± 1.22	x 94.0	x 66.7	x 1081

\*RipAY was activated by 8 μM *Af*Trx-h5.

\*\*Kumar *et al.*, (29).



FIGURE 1.

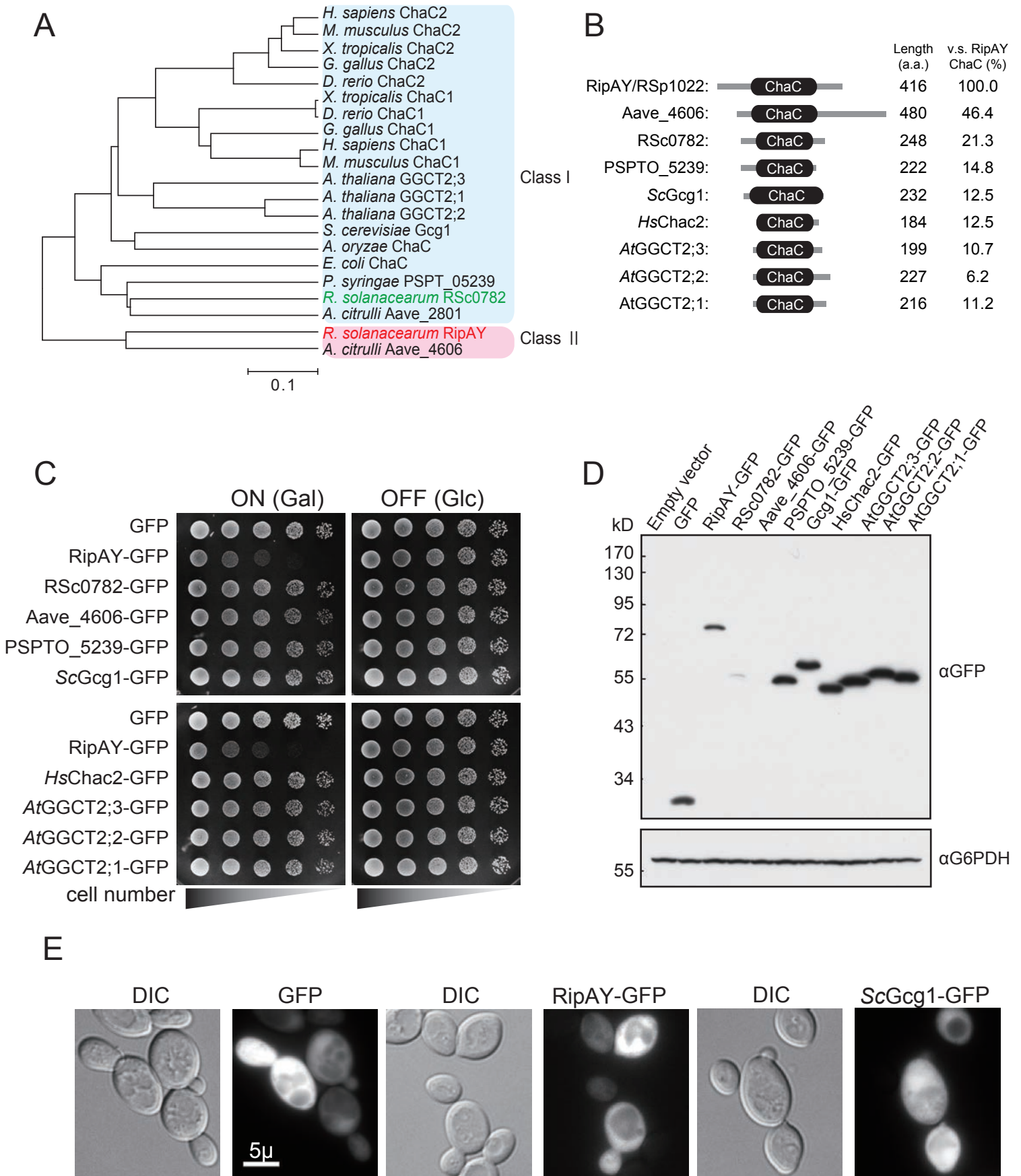


FIGURE 2.

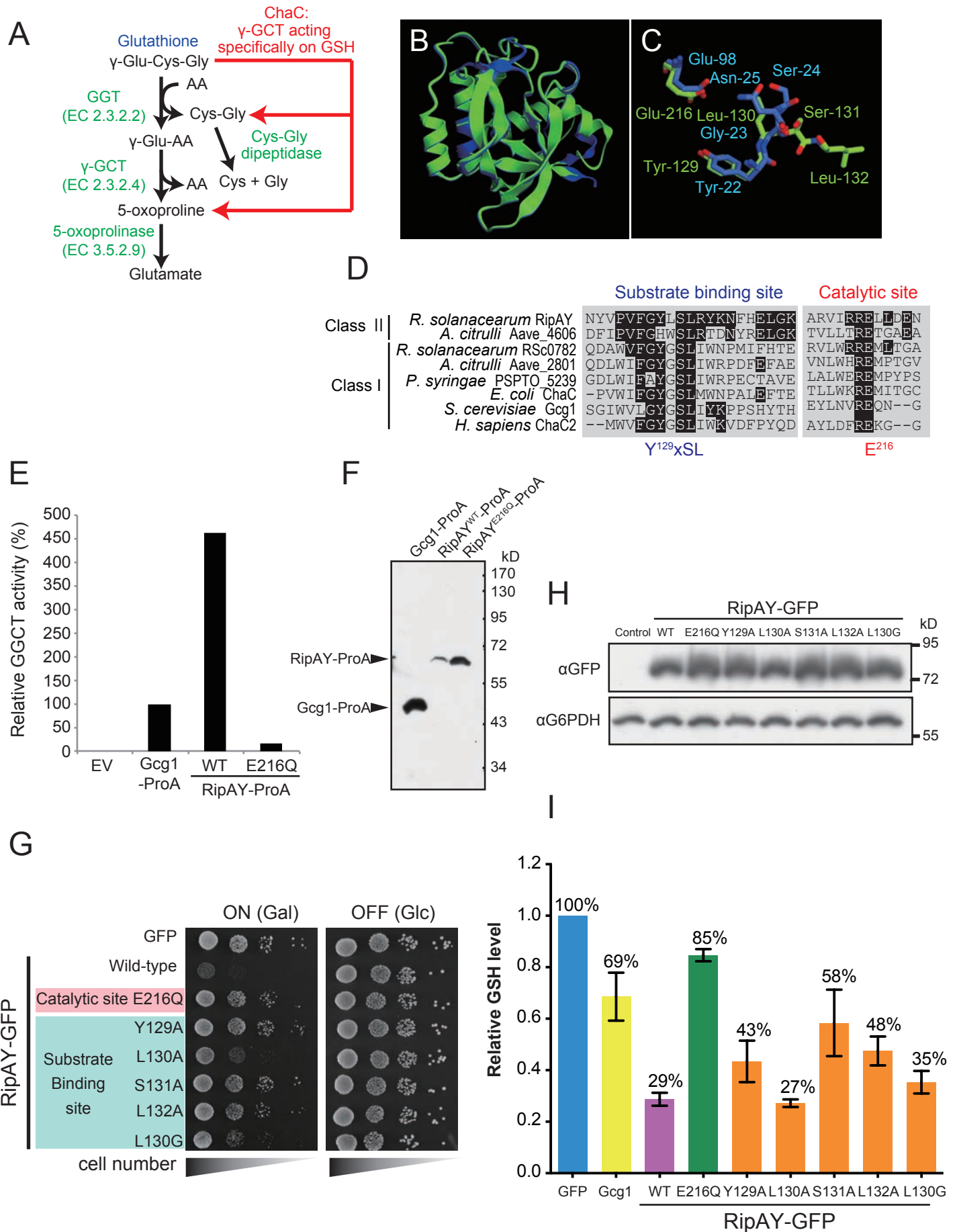


FIGURE 3.

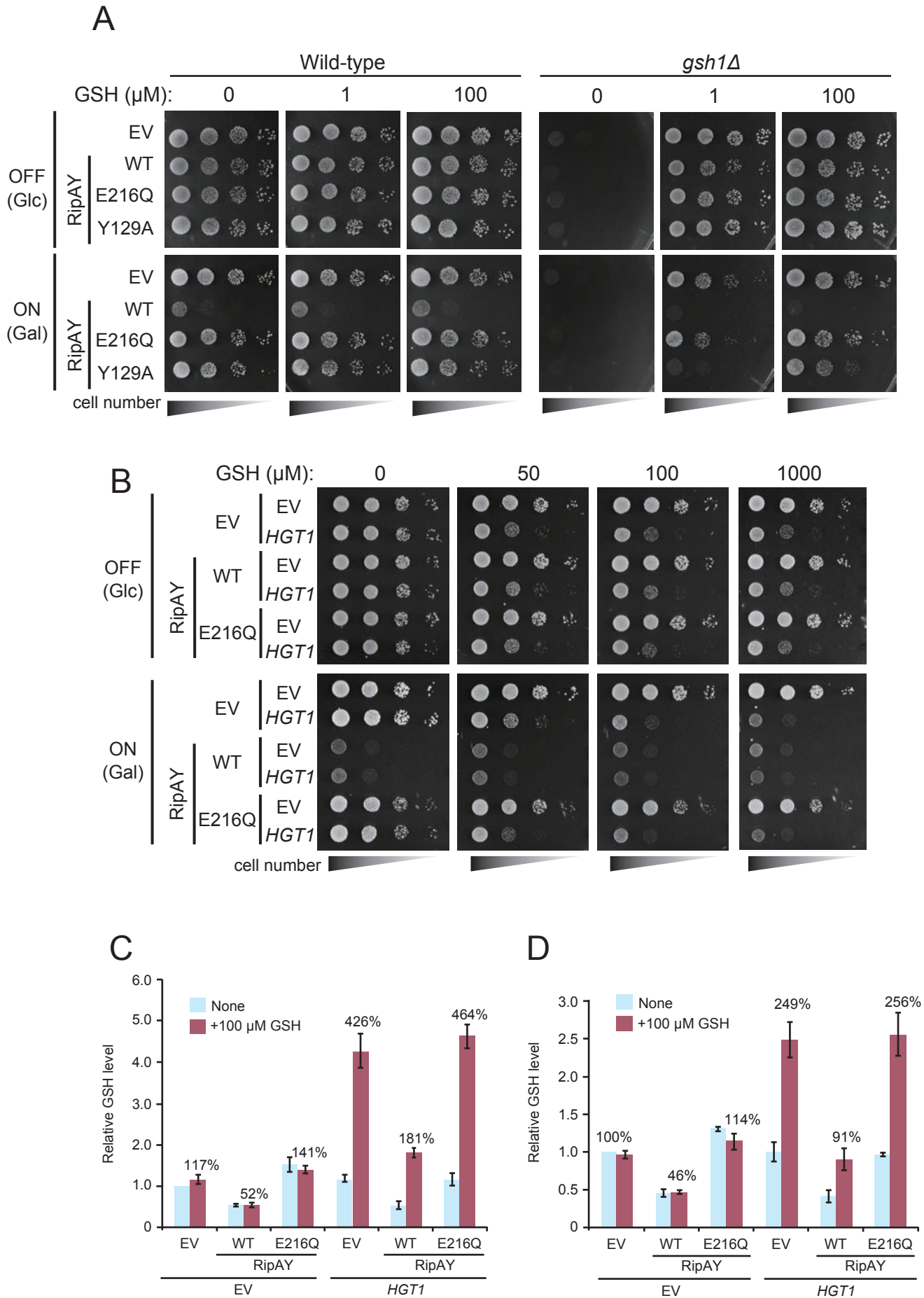


FIGURE 4.

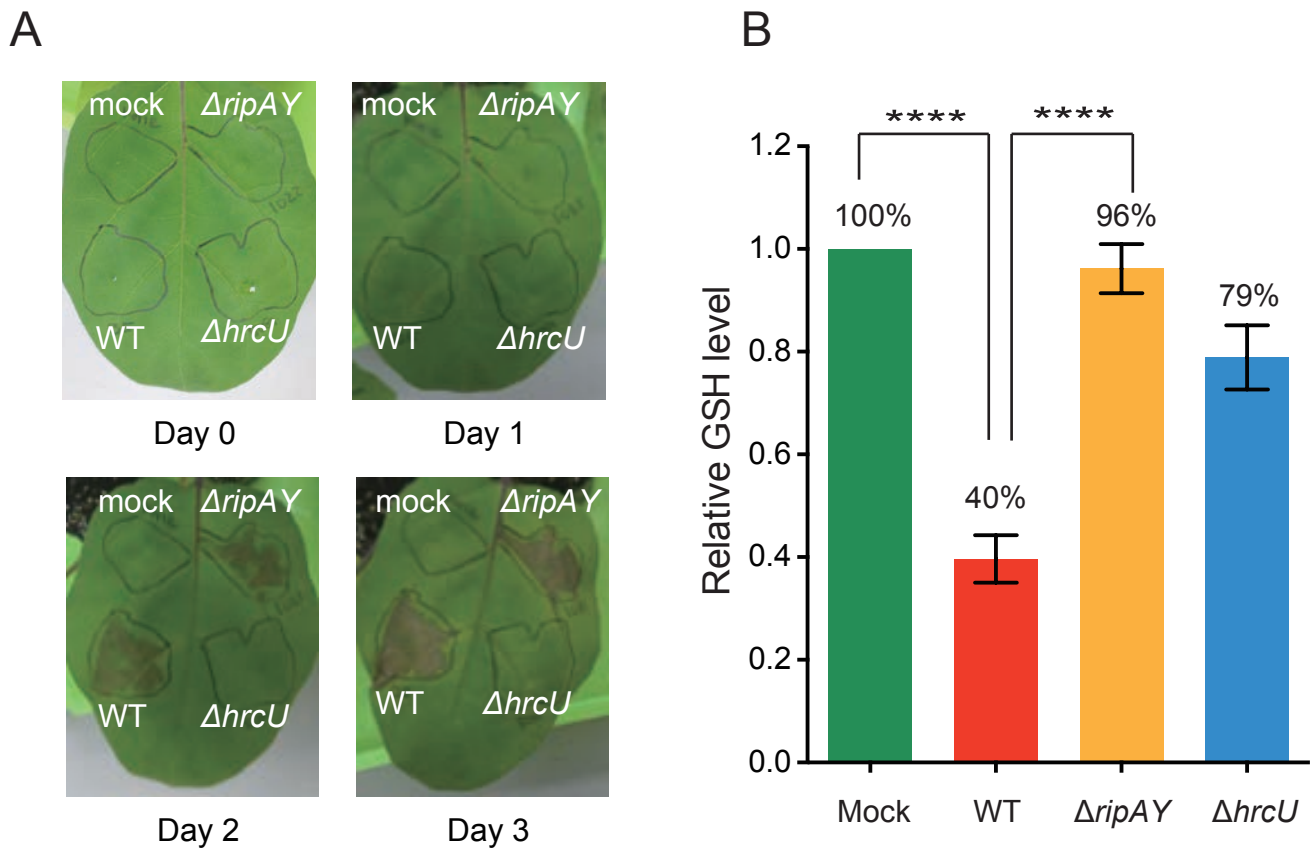


FIGURE 5.

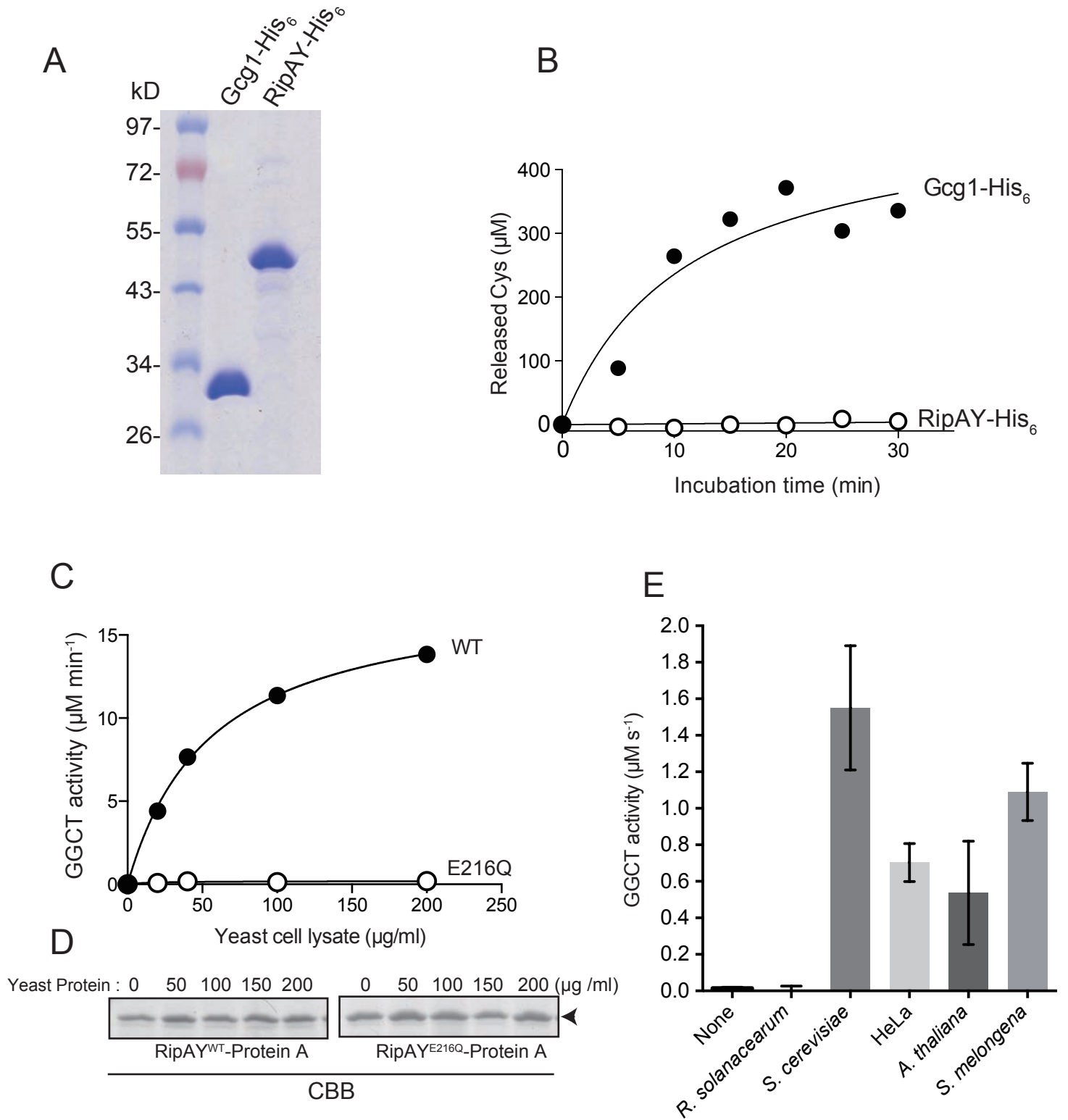
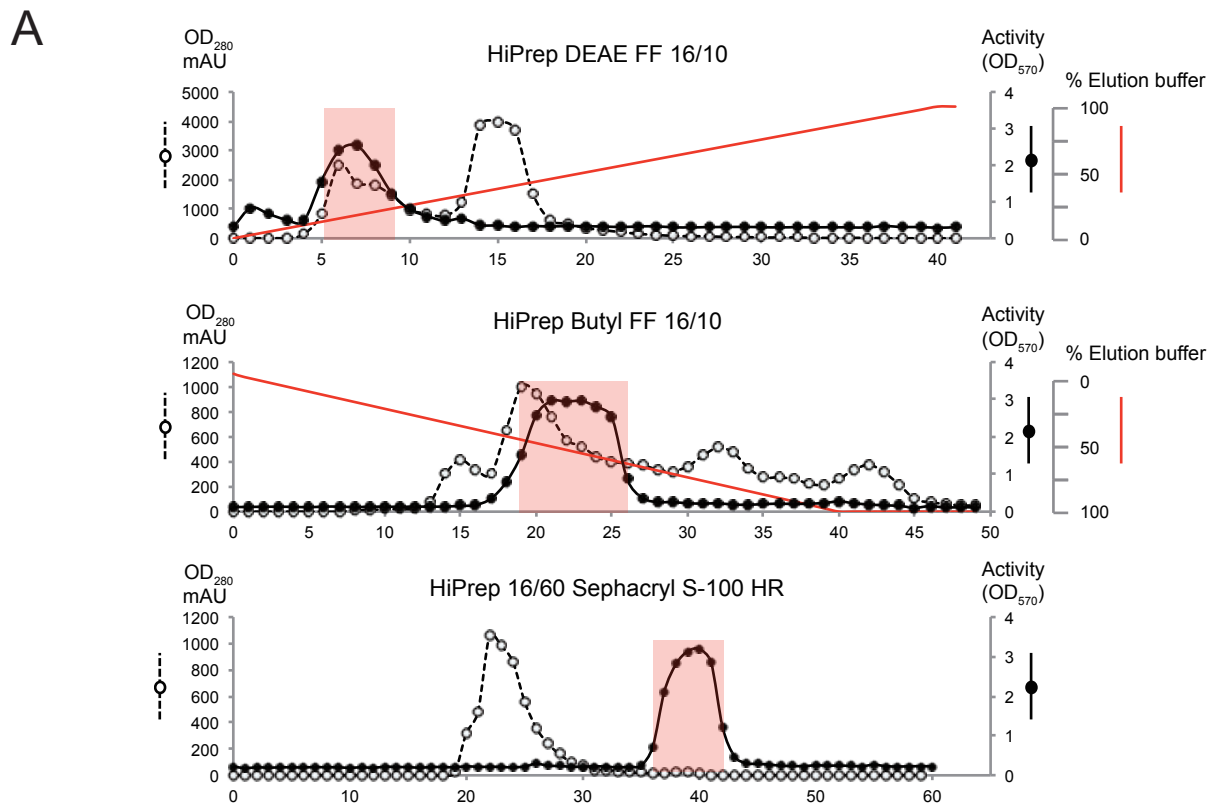
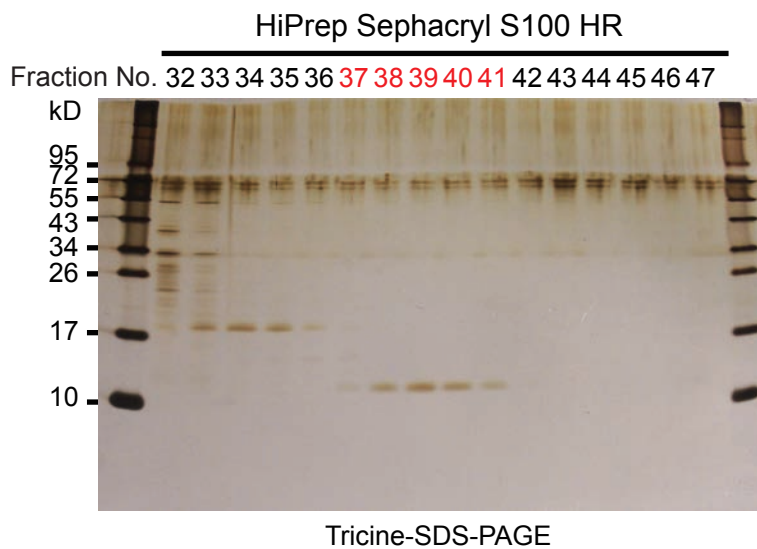


FIGURE 6.



**B**



**C**

*S. cerevisiae* Trx1

1 MVTQF KTASE FDSAI AQDKL VVDF YATWC GPCKM IAPMI EKFS E QYPQA DFYKL DVDEL  
 61 GDVAQ KNEVS AMPTL LLFKN GKEVA KVVGA NPAAI KQAI ANA

peptide 1  
 peptide 2  
 peptide 3

*S. cerevisiae* Trx2

1 MVTQL KSASE YDSAL ASGDK LVVVD FFATW CGPCK MIAPM IEKFA EQYSD AAFYK LDVDE  
 61 VSDVA QKAEV SSMPT LIFYK GGKEV TRVVG ANPAA IKQAI ASNV

peptide 4  
 peptide 5  
 peptide 6

FIGURE 7.

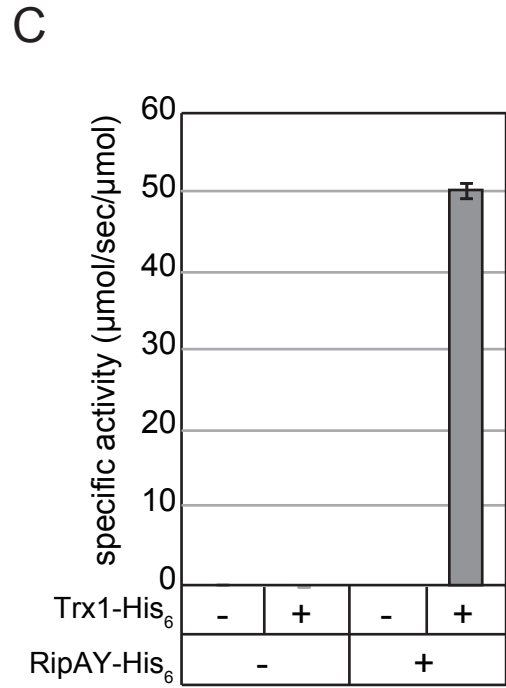
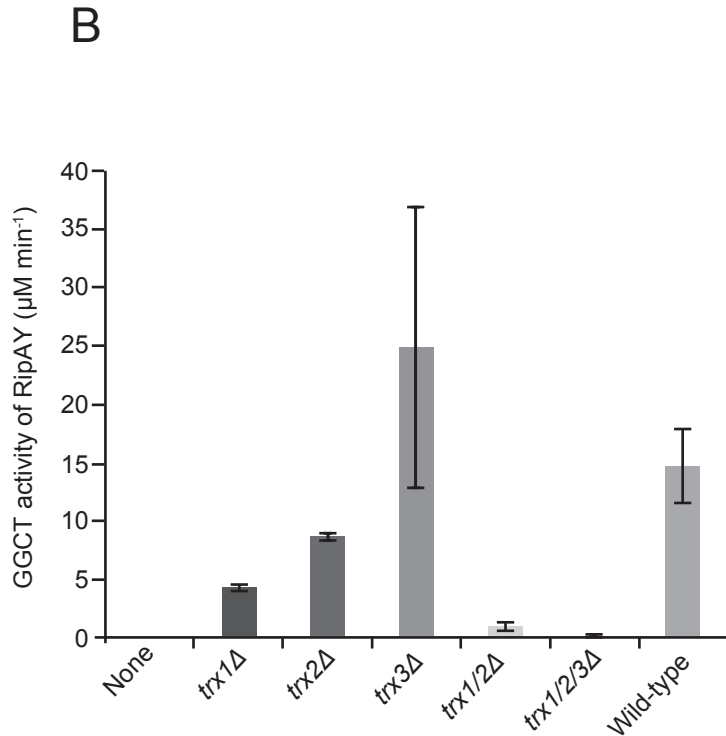
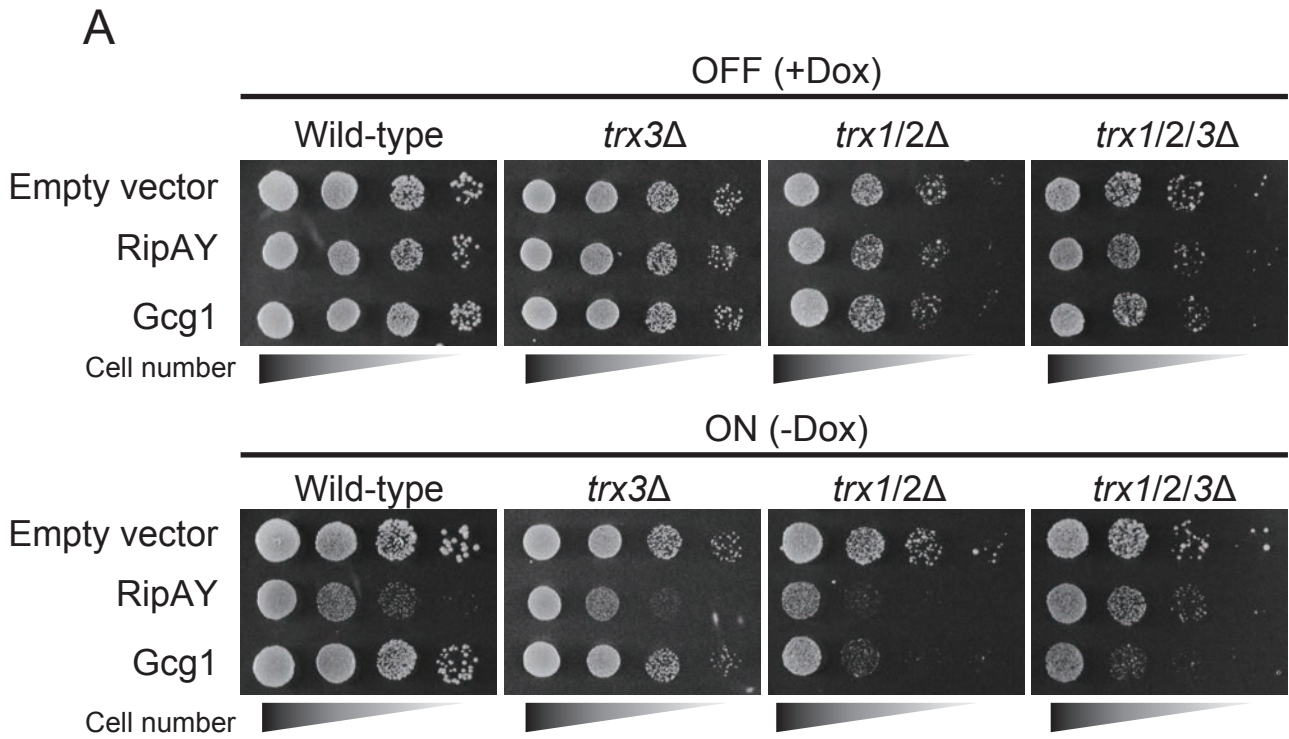


FIGURE 8.

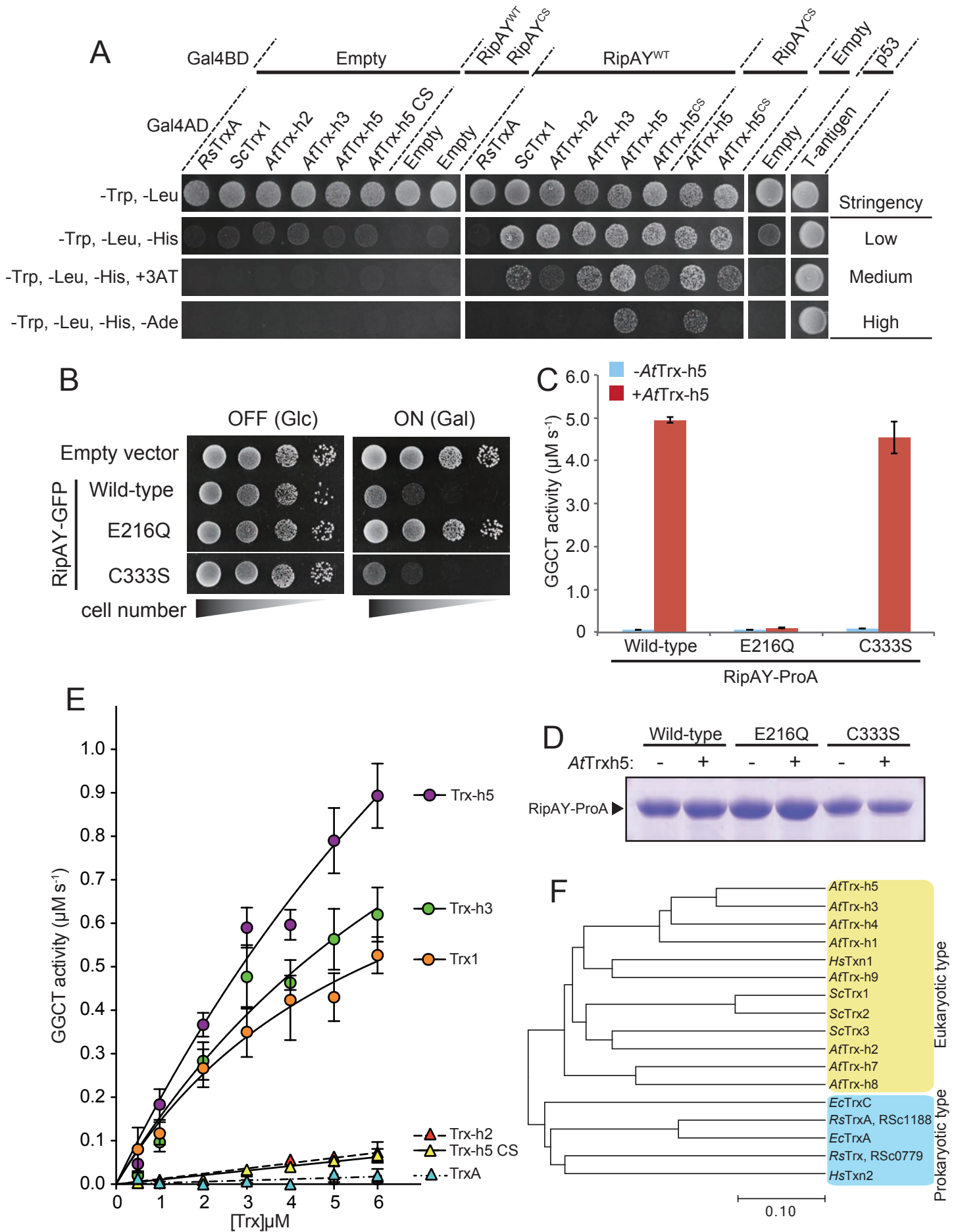




FIGURE 9.

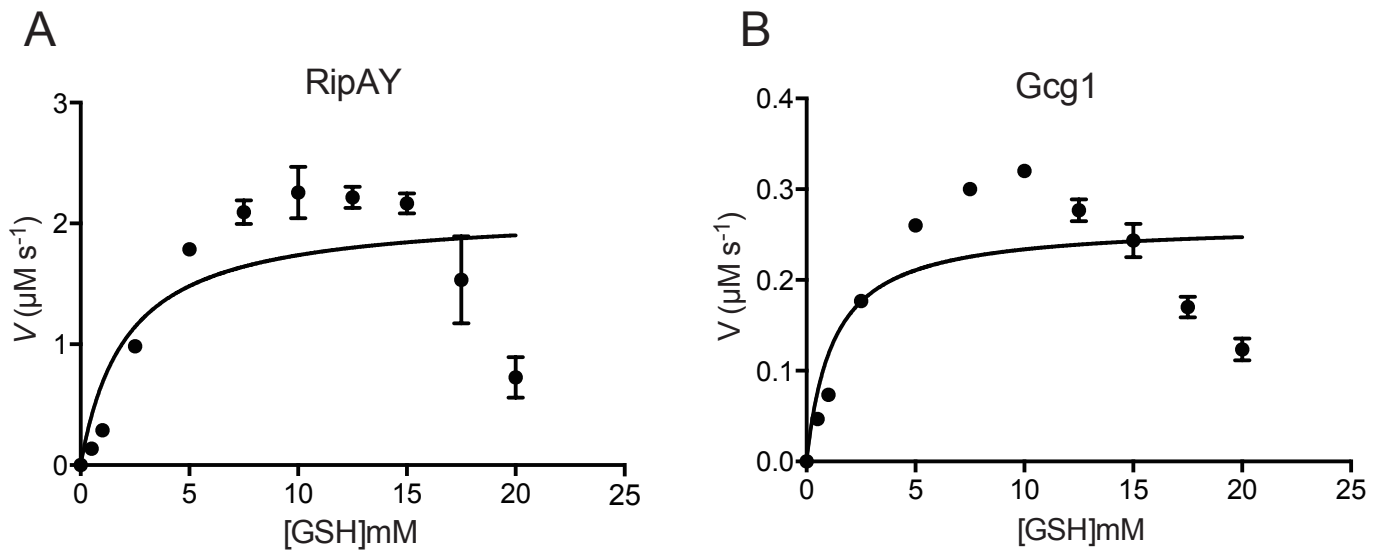
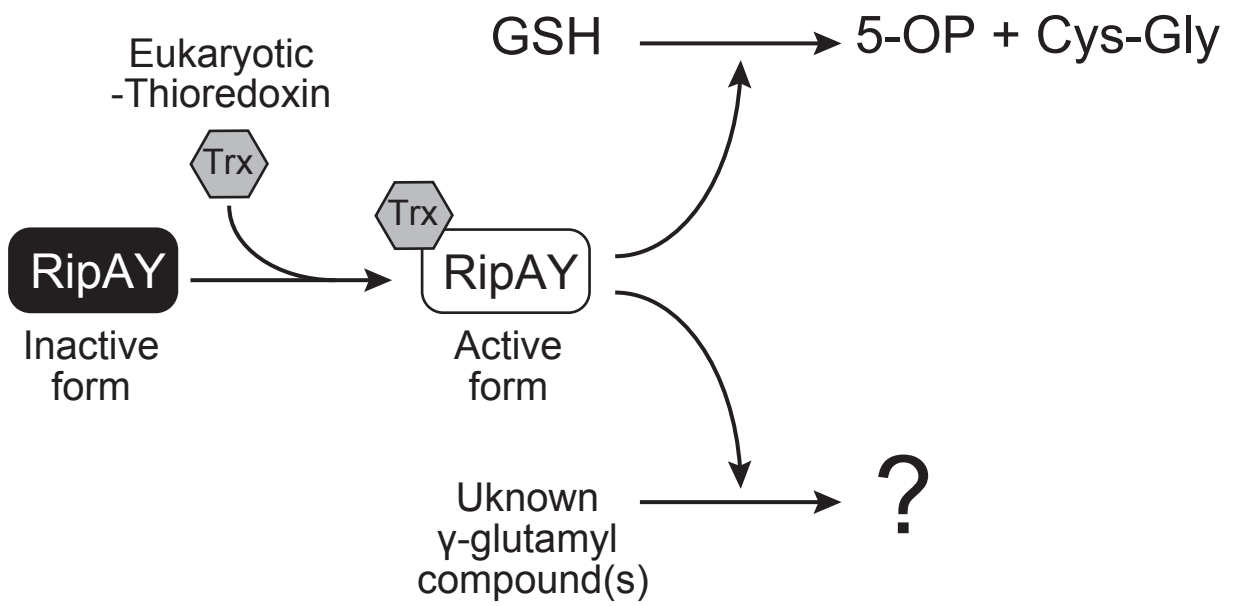


FIGURE 10.



**RipAY, a plant pathogen effector protein exhibits robust  $\gamma$ -glutamyl cyclotransferase activity when stimulated by eukaryotic thioredoxins**

Shoko Fujiwara, Tomoki Kawazoe, Kouhei Ohnishi, Takao Kitagawa, Crina Popa, Marc Valls, Stéphane Genin, Kazuyuki Nakamura, Yasuhiro Kuramitsu, Naotaka Tanaka and Mitsuaki Tabuchi

*J. Biol. Chem.* published online January 28, 2016

---

Access the most updated version of this article at doi: [10.1074/jbc.M115.678953](https://doi.org/10.1074/jbc.M115.678953)

Alerts:

- [When this article is cited](#)
- [When a correction for this article is posted](#)

[Click here](#) to choose from all of JBC's e-mail alerts

This article cites 0 references, 0 of which can be accessed free at <http://www.jbc.org/content/early/2016/01/28/jbc.M115.678953.full.html#ref-list-1>